Lung Tuberculosis Detection Model in Thorax Radiography Image

By. Jemal Ahmed

A Thesis Submitted to the Department of Computing in Partial Fulfillment for the Degree of Master of Science in Software Engineering

School Of Electrical Engineering and Computing
Department of Computing

Office of Graduate Studies

Adama Science and Technology University

Adama, Ethiopia
August 5, 2019

Lung Tuberculosis Detection Model in Thorax Radiography Image

By. Jemal Ahmed

A Thesis Submitted to the Department of Computing in Partial Fulfillment for the Degree of Master of Science in Software Engineering

School Of Electrical Engineering and Computing

Department of Computing

Office of Graduate Studies

Adama Science and Technology University

Adama, Ethiopia

August 5, 2019

DECLARATION

I hereby declare that this MSc thesis is my original work and has not been presented as a partial degree requirement for a degree in any other university, and that all sources of materials used for the thesis have been dully acknowledged.

Name: **Jemal Ahmed**

Signature:

This thesis has been submitted for examination with my approval as thesis advisor.

Name: **Mesfin Abebe (PhD)**

Signature:

Date of Submission: ______________________

APROVAL OF BOARD OF EXAMINERS

We, the undersigned, members of the Board of Examiners of the final open defense by **Jemal Ahmed** have read and evaluated his thesis entitled **"Lung Tuberculosis Detection Model in Thorax Radiography Image"** and examined the candidate. This is, therefore, to certify that the thesis has been accepted in partial fulfillment of the requirement of the Degree of **MSc in Software Engineering**

Dr. Mesfin Abebe	____________________	__________________
Supervisor/Advisor	Signature	Date
Dr. Tilahun Melak	____________________	__________________
Chairperson	Signature	Date
Dr.-Ing Frezewd Lemma	____________________	__________________
Internal Examiner	Signature	Date
Dr. Sudhir Kumar	____________________	__________________
External Examiner	Signature	Date

ACKNOWLEDGEMENT

First and for most, I would like to thank the almighty **Allah**. Then, I would like to extend my heartfelt and deepest sense of thankfulness to my advisor **Dr. Mesfin Abebe** for his continuous and open support, constructive comments, guidance and suggestions. I appreciate his dedication from the beginning to the end to teach me for the first time how to conduct and write a research. It is with his continuous follow up, encouragement and advice that this thesis came to realization.

I would like to take this occasion to express my deep appreciativeness to my families, friends and peers who, in one or the other way brought me up to a success in my academic endeavor, especially, my wife **Miss. Zeyba Abrar** for their endless moral support. I would also like to Wolkite University for sponsoring me to attend my second degree. I would like to thank all the staff members of the department of Computer Science and Engineering involved in the process, all Infor as well as my classmates for working together in different projects and assignments.

TABLE OF CONTENTS

LIST OF EQUATIONS

LIST OF ALGORITHM STEPS

LIST OF TABLES

LIST OF FIGURES

LIST OF ABREVIATIONS AND ACRONYMS

AI	-	Artificial Intelligence
AIDS	-	Acquire Immune Deficiency Diseases
ASTU	-	Adama Science and Technology University
AUC	-	Area Under ROC Curve
CADe	-	Computer Aided Detection
CADx	-	Computer Aided Diagnosis
CNN	-	Convolutional Neural Networks
CT	-	Computed Tomography
CXR	-	Chest X-Rays/ Radiography Image
DIP	-	Digital Image Processing
EM	-	Electromagnetic
GLCM	-	Gray-Level Co-occurrence Matrix
HIV	-	Human Immunodeficiency Virus
IMG	-	Vector Graphics File
JSRT	-	Japanese Society for Radiological Technology Dataset
LTBI	-	Latent Tuberculosis Infection
MC	-	Montgomery County Dataset
MRI	-	Magnetic Resonance Imaging
PA	-	Posterior-Anterior
PNG	-	Portable Network Graphics
RGB	-	Red, Green and Blue color spectrum
ROC	-	Receiver Operating Characteristic
ROI	-	Regions of Interest
SVM	-	Support Vector Machine
TB	-	Tuberculosis
WHO	-	World Health Organization
XOR	-	Exclusive OR

ABSTRACT

Tuberculosis (TB) is a communal disease with high death and disease rates worldwide. The chest radiograph (CXR) is commonly used in diagnostic solutions for lung TB. Automatic computer-aided solutions to identify TB using CXRs can advance the efficiency of the diagnostic of TB. In this study, an automatic TB detection model using CXR image is proposed. By identifying open issues from the current the state-of-the-art; how to detect the lung region automatically without any input like lung mask or model, and what are the features can identify a given CXR image is infected or normal are considered using three public datasets such as Schengen, Montgomery Country (MC), and JSRT set a total of 1047 CXR images. The proposed model used a new approach which is clear the intensities that interconnected with the border CXR image then continue to normal and further processes in image processing. The possible statistical textural features of a lung object is obtained from the first-order and second-order Gray Level co-occurrence Matrix (GLCM) statistical features. The performance of the proposed model was evaluated using accuracy, sensitivity and specificity. The model was achieved AUC 91%, 62%, 71%, and 81% on Schengen, JSRT, MC and Combined set respectively.

Keywords- Tuberculosis; pulmonary; chest radiography; computer-aided diagnosis; biomedical imaging; digital image processing

CHAPTER ONE

1. INTRODUCTION

1.1. Introduction

Digital image processing (DIP) has to turn into an important part of our modern lives. On every occasion an image is taken with a digital camera, a smartphone or a custom camera system formed for one or more industrial or scientific applications, so the image processing is involved. The capabilities of DIP are not restricted to improve the quality of pictures. But, DIP also able to support in every activity in business processes, scientific investigations and others. For example, doctors in the discovery or detection of diseases and able to assist in the protection of life and the prevention of human sickness related suffering uses such applications.

An application area of DIP in medical sciences is the development of computer-aided diagnosis (CADx) systems. These CADx systems evaluate for example an x-ray or computed tomography (CT) image's information and mark suspicious regions of interest (ROI) for additional investigation by radiologists. They are also able to identify whether the radiographic images are normal or abnormal. Although there are lots of modern alternative technologies to the x-ray imaging, like CT scans or Magnetic Resonance Imaging (MRI), it is still a broadly used tool for medical analysis. Especially the development of digital chest radiography (CXR) increased the acceptance of x-ray imaging for several motives like low implementation cost, medical price and became perceived as part of repetitive patient care [1].

TB is initiated by bacteria (Mycobacterium tuberculosis) that most often affect the lungs and also other organs such as heart, kidney, and brain. It is treatable and preventable but easily spread from person to person over the air when people with lung TB cough, sneeze, they release the TB microorganisms into the air. According to the 2017 WHO report [2] TB is the second prominent cause of death from an infectious disease besides HIV (Human Immunodeficiency Virus) and one of the top 10 causes of death worldwide, killing an estimated 1.3 million people and supplementary 0.4 million deaths causing of TB disease among people having HIV in 2016.

The incomparable growth of the TB epidemic in Africa is attributable to many factors, the most significant being the HIV epidemic. Though HIV is Africa's leading cause of death, tuberculosis is the commonest coexisting state in people who die from AIDS. Numerous analytical studies have presented such as 30 to 40% of HIV infected adults die from TB in Africa [3]. Especially in sub-Saharan Africa [4], improper density of radiologists at country level due to health professional migration to advanced countries, insufficient resource setting, and inadequate distribution of resources including human and material between destinations are important factors for TB infections.

Aside prevention and controlling mechanisms of TB, screening or diagnosis, which used to identify infected patients is an important task. For example, the skin test (inaccurate or wrong effects some time), sputum test (the test may stretch 4-8 weeks and have become fewer reliable in residents with a high occurrence of HIV/AIDS) and Chest radiographs (used to find TB in early stage within a short time which helps us to prevent death rate). Through the technology advancement, the current advancement [5] and achievement in the experiences of medical imaging practices assisted in inventing novel and innovative imaging techniques in the diagnosis of the patients by observing the human body internally and recognize different body parts for suspicions medical disorder [6]. However, human body structures that are concealed by tissues, bones, and skins but can be shown by x-rays and the abnormalities of blood vessels, airways, bones, lungs, and heart can be examined. Hence, the thorax radiography image also called digital Chest X-ray (CXR) that it works mainly based on observing and interpreting by radiologists who use the case with an input CXR, then simply comparing the two sides (left and right) of a lung image and if they observed any difference and abnormality they will announce as TB case or active case with TB. Obviously, this experts' decision may give wrong interpretation especially at the latent stage of the infectious. CXR is one of the most known diagnostic practices for cardiothoracic and lung disorders [7]. It is an initial examination tool that is commonly used in medical situations to notice defects in the cardio-thoracic area which contains heart and lung pathologies [8]. The various manifestation of TB on CXRs from diverse populations needs a system that can be altered to deal with diverse types of anomalies [9]. CXR is becoming gradually important in the fight beside TB because existing screening diagnostics such as sputum discoloration have developed less consistent in populations per a high occurrence of HIV/AIDS.

To come up above problems, researchers are introducing differential computer-aided diagnosis (CADx) systems via a digital image processing technique with CXR as inputs that used to support and change the manual TB screening or testing method with significant advantages. Similarly, in this thesis, an automatic TB screening model is proposed to detect the TB (especially at the latent stage) in the CXRs using digital image processing with the help of textural feature extraction method which is GLCM [10]. Beyond the solution proposal, it implemented using the three publicly available datasets and evaluated the model accordingly.

In this chapter, the basis of the study is described with the motivational aspects of the thesis in subsection *1.2*, the formation of problem statement in subsection *1.3*, definition of objectives of the study in subsection *1.4*, an overview of the methodological approach of the study also in subsection *1.5* , and accordingly, in subsection *1.6* and subsection *1.7* about the scope and the application of the study are described.

1.2. Motivation

Nowadays, every activity or service that might be owned by the individual, corporate, private or public organization is exercising or running by computer system technologies it may be partially or totally and the conversion process is also called computerization. Such technologies implements in many sectors include business, banking, insurance, education, marketing, healthcare, engineering design, military, communication, and government to automate or digitize their simple to complex activities in order to improve their performance and customer satisfaction or profit in general.

The health sector(can be primary, secondary, tertiary, quaternary, or community care) is one of the major sector to be automated its sections like patient information, tools and medicine information, medical practice information, and other technology-enabled activities such as CADx or computer-aided detection(CADe). In radiologic related services in the health sectors, CADx or (CADe) is a system and creates a viable alternative for medical imaging techniques like MRI, CXR, ultrasound, and CT scan reading. These systems can assist medical workers like doctors in the clarification of medical images plus possibly early disease detection.

The CADx or CADe can serve as an alternative resource in one or multiple levels probably not all just accountable for the final explanation of a medical image. The second interesting issue is the lack of human resources and radiological interpretation know-how weaken TB screening programs [3], especially in TB endemic countries. Plus to this poor judgment, inadequate skill and diagnostic errors can directly cause patient death and harm [11]. The third issue is making a reference model as a real machine learning principle which is taking learning capabilities from past events and making an appropriate decision. The last issue is that an automatic examination and classification of CXR can be used as a consistent alternative to more refined and technologically demanding techniques (like sputum smear or culture check).

In order to overcome all the above issues, acquiring mass screening capabilities, improving the detection, and developing relatively an accurate and automatic model are initial motivation corners for this study. Hopefully, the study will support TB screening method in the level of the case that the infection mainly at the latent (non-infectious) stage before its disease (infectious) stage.

1.3. Statement of the Problem

TB is an airborne disease, triggered by the bacterium Mycobacterium TB (MTB) [12]. MTB is carried in airborne spots, called droplet nuclei, about 1– 5 microns in diameter. Infectious droplet nuclei are produced when persons who have a lung TB disease cough, sneeze, shout or sing; and infection happens when a person gasp droplet nucleus holding tubercle-bacilli that spread the alveoli of the lungs. Unfortunately, persons with latent TB infection (LTBI) have M. tuberculosis in their bodies, but do not have TB disease and cannot feast the infection to others and persons who have TB disease may feast the bacteria to others.

LTBI and TB disease [12] has their own relative characteristics includes ***1)*** it has a small amount of TB bacteria in the human body that are alive, but inactive vs. has a large number of active TB bacteria in human body, ***2)*** cannot spread TB bacteria to others vs. may spread TB bacteria to others, ***3)*** does not feel sick, but may become sick if the bacteria become active in the human body vs. may feel sickening and may have signs such as a cough, fever, and/or weight loss, ***4)*** usually has a TB skin test or TB blood test reaction indicating TB infection vs. usually has a TB skin test or TB blood test reaction indicating TB infection in similar way, ***5)*** radiograph is typically normal vs. radiograph may be abnormal, ***6)*** sputum smears and cultures are negative vs. sputum smears and cultures may be positive, ***7)*** should consider treatment for LTBI to prevent TB disease vs. needs treatment for TB disease, ***8)*** does not require respiratory isolation vs. may require respiratory isolation and ***9)*** not a TB case vs. a TB case respectively.

Based on explanations given above, can identify numerous problems, for example, inactive TB bacteria, but may in small number, no symptoms, may not spread to others, inaccurate test result plus time stretch, normal radiograph result, negative sputum, prevention opportunities and not a TB case. This implies, aside prevent the death needs to work on spreading of the infection.

To get relative solutions towards such problems, this study is formulated with the support of the following three research questions:

Q1. *How to define the lung region from CXR image?*

Q2. *What are the features of the proposed model?*

Q3. *What are the important parameters that can be used to measure the performance and the applicability of the model?*

1.4. Objectives

This proposed study has a general and specific objectives which are outlined below.

General Objective

The general objective of the study is to design an automatic machine learning model for pulmonary TB detection.

Specific Objectives

To achieve the general objective stated above, the following specific objectives are stated.

- To analysis and find the state-of-the-art, principle, and technologies of actual problem's environment and other domain related proposed method.
- To define the necessary lung region.
- To propose a reference model for TB detection in CXR image.
- To implement the proposed model.

- To test and evaluate the performance with the applicability of the model.

1.5. Methodology

To fulfill the desired aim of the study, the following four characteristics or sections are defined accordingly with the help of Design Science research methodology approach. This approach is suitable for the proposed model because of the proposed model is initiated from the current context on TB detection in CXR image. To achieve the objectives of the study, the following procedures were applied.

Literature Review

To answer the first specific question and indirect answering for question other than the first one via related work study, selecting as well as examining current knowledge already proven by researchers is one of the main task for such proposed technical study and it should be analyzed strategically. Due to this, the selection of the source of literatures, selection processes and extraction techniques were followed.

Dataset

The CXRs dataset is the only data that can be used in this proposed model. But it is difficult to get the dataset(s) locally because of limited perception by health care organizations and limited source in terms of technology and data persistence habit. Furthermore, in most of the similar articles were used common and public datasets.

Due to this, the two public datasets reported [13] are considered. The first one is the Montgomery **County chest X-ray set (MC)** has 138 frontal chest X-rays with the size of either 4,020×4,892 or 4,892×4,020 pixels and Portable Network Graphics (PNG) format as 12-bit gray level images, which 80 are normal cases and 58 are cases with signs of TB. Also, the second set is the **Shenzhen chest X-ray set** has 662 frontal chest X-rays with PNG format and the size can vary, but approximately 3K × 3K pixels.

Design

The proposed model which is an automatic TB detection model in CXR image used the model-based techniques. The major aspects of the model include ***1)*** preprocessing (image lung field detection, and masking), ***2)*** segment the lung region from the original image, ***3)*** the extraction of the potential textural features with the required processes ***4)*** evaluate the performance of the proposed model in CXR images.

Procedures

The followings are sequences of major tasks followed for the proposed model:

Task 1. Literature study related to the actual case environment

Task 2. Collection of a suitable development image dataset.

Task 3. Identifying requirements for the model.

Task 4. Methodology definition to derive the model according to requirements.

Task 5. Development of the model.

Task 6. Model verification according to the requirements.

Task 7. Documentation or thesis report.

Implementation Tools:

With the help of MATLAB programming language that it is applicable to perform many operations and methods on the patient's CXRs for better and accurate results. And others relevant materials and expenditures are also listed in subsection *3.8*.

Performance Evaluation

To examine the performance of the proposed model was evaluated using standard measurement matrices such as: accuracy, sensitivity, and specificity.

1.6. Scope and Limitations

Scope of the study

The study is focused on an automatic TB screening or diagnosis in CXR image only rather than other screening mechanisms like skin test, sputum test, and patient's historical or oral events.

Limitations of the study

This proposed study will face different constraints (limitations) while working the study. These could affect the solution to get its better performance, applicability and usability. The following major limitations or constraints were affected the entire study.

- The variability of the dataset's profile e.g. intensity values and unappropriated cropping of CXR images during preparation of datasets.
- Horizontal clinical and individual information, especially, age group will not be considered, but it is an encouraging part of TB screening as long as CXR imaging for the performance of the overall screening.

1.7. Application of Results

We expected that the thorax reference model could provide different benefits to the target populations in the identified domain area. After evaluation of the results found in this thesis, the following are major stakeholders could be a beneficiary.

- Researchers who intended further study in the area as the state-of-the-art.
- Any health sector organization, especially, unavailability of radiologist or CXR imaging experts in the organization and TB infection diagnosis at its latent stage.
- Individual and the community in general, because of possible to screen the case before reaching its spread stage.

1.8. Document Structure

This thesis report has seven chapters including this current. Chapter 1 introduces the basics of the thesis work from the statement of the problem to the application description with introductory information. Chapter 2 presents the fundamental information of the study as literature review and also the brief of best relevant articles as basis of the proposed solution. In chapter 3 the new methodological approach is presented for the detection of TB, based on the results of the literature research. Chapter 4 describes the proposed model with appropriate steps of working. Chapter 5 describes the implementation of the proposed model. Chapter 6 highlights the result from the implementation with the triangulation of the state-of-the-art. In the last chapter, the conclusion and recommendation from the thesis with open issues as a future work are stated.

CHAPTER TWO

2. LITERATURE REVIEW AND RELATED WORKS

2.1. Introduction

The beginning of image processing methods times back to the late 1960s and early 1970s and was used in medical imaging, astronomy and remote earth resources observation. Meanwhile, digital image processing has been growing dynamically. Other application areas are now using digital image processing techniques for example in robotic vision, product inspection, and scientific research [14].

In this chapter, the background information of the study was discussed related to the context of the study. Primary, from the social context side the medical diagnosis, and TB & its screening techniques and it has subsections contains about TB, the types & stages, the pathology, the diagnosis and the challenges of the pulmonary TB was documented. Then, the technical context side also the medical image analysis, computer vision and image processing representation, machine learning were discussed.

This chapter is structured into five subsections: medical diagnosis, TB and its screening mechanisms, medical image analysis, image processing representation and machine learning.

2.2. A Brief Overview of Medical Diagnosis

Preventive medication can be characterized as primary, secondary, or else tertiary [15]. Primary prevention goals to eliminate or decrease disease threat factors or vulnerability. For example, vaccination, giving up or not starting something to the danger that used in activities or actions for both individual and public. This method is focusing on reducing the danger of contact to a risk factor or health cause in an individual or the population. It also includes both health promotion and specific safeguard as modes of mediation. Meanwhile fruitful primary prevention aids escape the suffering, cost, and load related to the disease, it is usually considered the greatest economical form of health carefulness.

Secondary prevention practices inspire timely discovery of disease or ancestor states at the subclinical stage. For example, Pap smear to detect certain biological infections, measurement of blood pressure. Such methods focus on the subclinical and the early clinical stage. These methods enable early detection and prompt effective intervention to correct departures from a state of health. It includes screening and early diagnosis. With initial case finding, the usual history of a disease or how the sequence of a sickness unfolds over time without action can often be changed to minimize suffering and maximize well-being.

Tertiary prevention measures contain the caution of established disease, with efforts made to restore to maximum function, minimalize the dangerous effects of a disease, and avoid disease correlated difficulties. Since the disease is now recognized, primary prevention actions may have been ineffective. Initial detection may have minimized the impact of the disease over secondary prevention. Beyond these above levels of preventive medication, developing population centered information systems create it highly probable to combine prevention and caregiving that new attention on the opportunities for realizing well and more reasonable delivery of healthiness [16].

The tool for supplementary examination is focused on the level of the competence where the action takes place [15]. Once there is no test center available, either for outpatient or inpatient care, fast analysis tests may be made obtainable (for malaria, HIV, etc.). A laboratory and material necessity be a system for certain diseases, such as TB.

Therefore, the secondary prevention mechanism can be automated for early detection and diagnosis when if the occurrence of primary prevention is unsuccessful. In the next section, the brief of TB and its screening mechanisms is documented.

2.3. TB and its Screening Mechanisms

According to the World Health Organization (WHO) [2], TB is the second most communal cause of death in the globe along with HIV/AIDS. A great occurrence of TB anywhere in the world poses dangers to the healthiness of people elsewhere, meanwhile, TB is spread by air. While the application of current knowledge and methods for the diagnosis, handling, and prevention of TB can create an influence [17]. In this subsection, a brief overview, the types, and stages (latent to infectious stages), the pulmonary TB, the diagnosis, and some basic challenges in terms of nature and diagnosis of TB has been presented.

2.4. Tuberculosis

TB is a highly contagious, persistent disease caused by the development of tough soiled nodules, or tubercles. The disease is most often produced by the bacterium Mycobacterium TB; typically happens in the lungs, but it also can spread to the other organs like skeleton or bone. Since its signs and symptoms are simply confused with those of many other mainly respiratory diseases, TB can be hard to diagnose and this clues to the importance of medical imaging for TB diagnosis. The communal symptoms of TB are cough, night sweats, chest pain, and breathlessness [18].

In general and radiological point of view [19], TB has exposed a renaissance in non-endemic residents in current years, a case that has indorsed to influences such as increased relocation or migration and the HIV widespread. While the thorax is most often involved, TB may involve any of a number of organ systems (like respiratory, central nervous, cardiac, gastrointestinal, musculoskeletal, and genitourinary systems), and appropriate analysis of the disease is extremely risky and challenging, meanwhile, late action is allied with severe sickness.

2.5. Types and Stages of TB

TB can be characterized into pulmonary and extra-pulmonary [18] and summarized in brief as follows:

2.5.1. Pulmonary TB

Lung (pulmonary) TB is a bacterial infection as a consequence of Mycobacterium TB, easily feast by airborne. Once contaminated, Mycobacterium TB multiplies gradually in the pulmonary and this characterizes the primary infection. Typical medical sorts in terms of symptoms and signs connected with lively lung TB are contained fever, cough, weight loss, hemoptysis, night sweats, fatigue, and chest pain.

According to Health Communities [18], pulmonary TB has different types includes TB pleurisy, primary TB pneumonia, miliary TB, cavitary TB, and laryngeal TB.

a) Primary TB Pneumonia

Such type of TB offerings as pneumonia and is very transmittable and rarely occurred. It happens most frequently and particularly young children and the aging with high productive cough and fever.

b) TB Pleurisy

This typically grows rapidly after primary infection. A granuloma positioned at the side of the lung separations hooked on the pleural space, the position between the lungs and the chest partition. Regularly, a couple of liquefied can remain to reproduce in the pleural space. After that the amount of liquefied growths radically and compresses the lung, producing shortness of breath, low-grade fever, and chest pain. TB pleurisy usually recovers without treatment; but, 2/3 of patients over TB pleurisy grow lively pulmonary TB indoors 5 years. Such type of TB can be observed in a CXR that shows significant amounts of liquefied around the space.

c) Cavitary TB

It includes the upper lobes or parts of the lung. The bacteria reason progressive lung damage by making cavities, or bloated air spaces and can rarely occur rapidly after primary contagion. Symptoms comprise night sweats, productive cough, fever, weakness, and weight loss. Here may be hemoptysis i.e. coughing up blood.

d) Miliary TB

It is easily dispersed and can occur just after primary contagion. The patient develops highly harsh with a high fever. The disease also may clue to continuing sickness and slow decline.

Symptoms may comprise night sweats, fever, and weight loss; can be hard to identify because the early CXR may be usual.

e) Laryngeal TB

It can contaminate the larynx and extremely infectious. Dysphonia is a primary symptom of laryngeal TB.

2.5.2. Extra pulmonary Tuberculosis

This kind of TB happens mainly in immune cooperated patients. For example, *lymph node disease* (making the lymph nodule to become enlarged and can produce a fistula), *TB peritonitis* (causing for coatings of the intestines and the coatings inside the wall of abdomen, generating mass fluid), *TB pericarditis* (can cause for the space between the heart and the pericardium to fill by fluid, delaying to fill with blood and beat ability of the heart), *osteal TB* (can cause for the contagion of any bone e.g. spine), *renal TB* (can cause asymptomatic pyuria and can feast to the reproductive tissues and interrupt reproduction), *adrenal TB* (causing for adrenal insufficiency in adrenal glands that increase steroid production in time of stress, and lead collapse and weakness), *TB meningitis* (it can contaminate the meninges and causes for devastating, foremost to permanent damage and death).

2.6. Anatomical Pathology of TB

Many structures of the chest are willingly observable on a CXR, but others, are difficult to see. Thus, the anatomy of CXR, lung abnormalities as TB with possible TB stages [20] are presented in *Table 2.1* below.

Table 2.1. CXR-anatomy and lung abnormalities

Manifestation Stage	The Anatomy	Findings	Finding's description
Anatomy of normal CXR image			▪ 1 - Trachea ▪ 2 - Hila ▪ 3 - Lungs ▪ 4 - Diaphragm ▪ 5 - Heart ▪ 6 - Aortic knuckle ▪ 7 - Ribs ▪ 8 - Scapulae ▪ 9 – Breasts ▪ 10 - Bowel gas

Manifestation Stage	The Anatomy	Findings	Finding's description
Primary TB	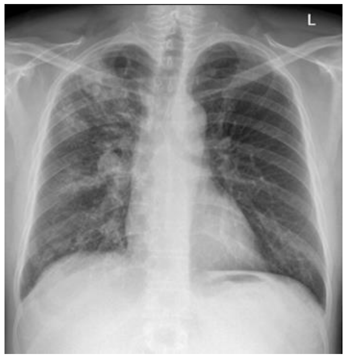	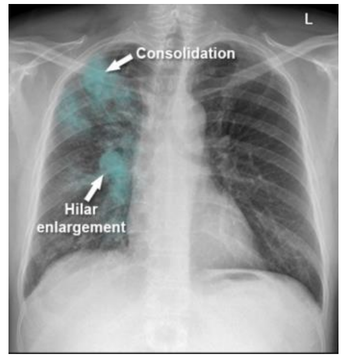	▪ There are no radiological features at this stage but a CXR may provide some clues to the diagnosis. ▪ The consolidation of the upper zone with ipsilateral hilar enlargement is typical features of primary TB.
Healed primary TB	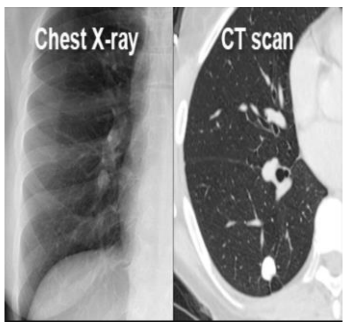	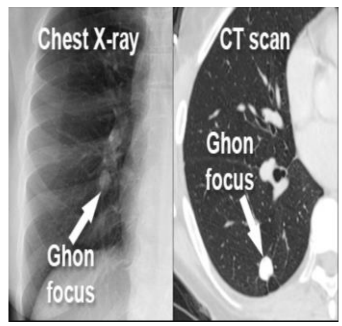	▪ An immune response to primary contagion, which forms the 'Ghon focus' – TB has gone! ▪ This CXR shows a large, rounded solidified focus near the right hilum.
Post-primary TB		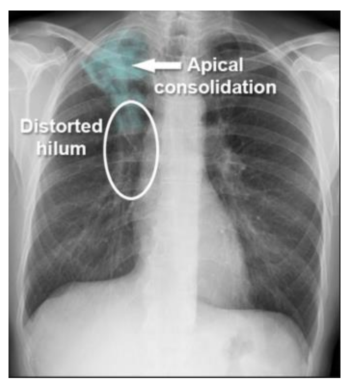	▪ Post-primary TB (secondary TB) is more common in immunocompromised individuals. ▪ The upper lobes are more commonly affected and the consolidation often extends to the hilum. ▪ The hilar structures are distorted due to volume loss of the upper lobe.

Manifestation Stage	The Anatomy	Findings	Finding's description
Post-primary TB-Lung cavity			▪ (Same patient as the image above (Post-primary TB) – 4 months later). ▪ Cavities are a common finding in mycobacterial contagion.
Healed Post-primary TB		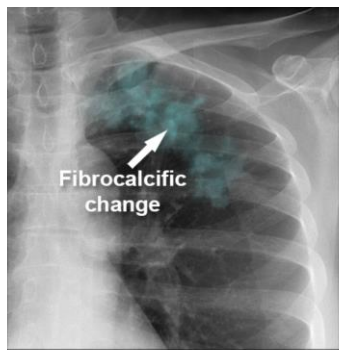	▪ An immune response to post-primary infection, the affected region often becomes scraped (fibrotic) and solidified. ▪ The combined fibrosis and solidification can be described as 'fibro-calcific change'.
Miliary TB		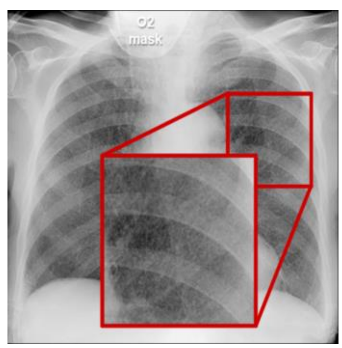	▪ Miliary TB is due to the dispersed spread of mycobacterial infection. ▪ It can occur either at the time of primary infection or on disease reactivation – prognosis is poor. ▪ Very fine nodules are typically seen scattered throughout the lungs.

2.7. Diagnosis

Based on the nature of TB, the symptoms and signs will differ between types [7] as stated in *Table* 2.2. Physical checkup encounters related to TB be subject on the tissues difficulty and complicated. Patients with pulmonary or lung TB may have abnormal breath resonances and respiratory breath signs. Similarly, signs of extra-pulmonary TB vary rendering to the tissues complicated and may include confusion, coma, neurologic deficit, lymphadenopathy, and cutaneous lesions.

Table 2.2. Possible symptoms for each type of TB

Type	Symptom
Meningitis TB	– headache - demanding for 2-3 weeks – understated mental status variations – lacking fever
Skeletal TB	– back pain or rigidity – lower fringe paralysis – joint pain- like knee, after that the ankle, elbow, and wrist
Genitourinary TB	– flank pain – dysuria – frequent urination, – a painful scrotal mass, prostatitis, orchitic, or epididymitis in men and – mimicking pelvic sickness in women
Gastrointestinal TB	– non-curative sores of the mouth or anus – trouble swallowing – abdominal discomfort with gastric infection – malabsorption with infection of the small intestine and diarrhea

Correct and appropriate diagnosis is the first step for starting actual handling for TB and interfering transmission or infectious. In order to diagnosis TB, there are a number of approaches much time with a combination of two or more techniques. The techniques include *careful history* (TB interaction and symptoms dependable with TB), *clinical examination*, *tuberculin skin analysis*, *CXR*, *bacteriological validation*, *inquiries relevant* for supposed pulmonary TB and supposed extra-pulmonary TB, and *HIV testing*.

2.8. Challenges

TB is hard to diagnose since the signs and symptoms are alike to those produced by other diseases like lung cancer, pneumonia, allergic bronchopulmonary aspergillosis, sarcoidosis, allergic alveolitis, pneumoconiosis, silicosis, anorexia nervosa, diabetes mellitus, hyperthyroidism, and Mediastinial.

The challenges during TB test or diagnosis and can be non-technical or technical [21].

Technical aspects:-

- Antibody information in patients through active TB overlay with patients with presumed latent TB infection (a significant facet of TB control in low drain locations),
- Antigens can be differentially stated in different body sections,
- Overlap TB symptoms with others' diseases symptoms like coughing and night sweet,
- Test correctness may vary in HIV infested against uninfected individuals and individuals with pulmonary alongside extra-pulmonary TB,
- HIV infected individuals,
- Samples like saliva or sputum may not be willingly available, and
- Lack of appropriate or incomplete antigenic targets are some issues included under technical aspects.

Non-technical aspects like the absence of information on target item profiles, private investment, supervisory standards and funding for developing are some examples and the aspect is not interesting for the intended objective, unlike the technical aspect.

2.9. A Brief Overview of Medical Image Analysis

Medical images are different from other images in that they show dispersals of several bodily features measured from the human body. Besides, analysis of such images is directed by very explicit outlooks which provided growth to obtaining the images in the primary place. This has significances on the kind of examination and on supplies for algorithms that convey out some or all of the examination. Developing an examination technique does not mean that the whole thing has to be formed from scratch. Different kinds of systems significantly support speedy system or software development are viewer system, analysis system, rapid prototyping system and system libraries [22].

Viewer software or system has been mainly settled to look at the facts, but frequently encloses some methods for analyzing the facts as well. Although it is not assumed to be stretched, it enables the advance of a new analysis technique by providing speedy access to the image facts. Analysis software is different from viewer system in that it is expected to offer the user with a set of parameterize-able analysis components that achieve different stages of image analysis going from image enhancement techniques to segmentation, registration, or classification tools.

The rapid prototyping programming language such as MATLAB is interpreter language that is tailed to rapidly processing arrays. It is suitable to be used for working with 2d plus 3d image arrays. It is possible to write programs that can be executed later. As with the prototyping languages, the open source libraries may be all that is needed to solve an analysis problem. But even if not, they will provide for quick access to methods that can be tested with respect to their capability for solving the problem. They also may provide state-of-the-art approaches to preprocessing, data access, and post-processing.

Medical images are pictures of distributions of bodily characteristics taken by an image acquisition equipment or system. Most of today's images are digital and come in one of two methods i.e. projection images project a bodily parameter in the human body on a 2d image and slice images make a one-to-one plotting of the measured value in a 2d slice.

In order to acquire digital imaging, there are four main and numerous minor imaging methods meet the above requirements. The main techniques are the CXR measures absorption of shortwave electromagnetic waves, the MRI measures density and molecular binding of selected atoms, the ultrasound captures reflections at boundaries between and within tissues and the nuclear imaging measures the distribution of radioactive tracer material administered to the subject. Other imaging techniques include the electroencephalogram (EEG) or magneto-encephalogram (MEG) imaging which is the record of brain electrical or magnetic fields respectively, optical and electron microscopy, optical coherence tomography, and photography.

Nowadays, Image analysis is becoming an important part of the clinical or medical workflow that needs to support the advance and carrying out better to ever.

2.10. Image Processing and Machine Learning

Basically, computer vision is related to image processing in the sense that the computer vision front-end is comprised of image processing techniques such as noise reduction, whitening or image enhancement. The machine learning on the other side is flexible as it can be used in either computer vision or image processing. Although each discipline has its own goal even if the relationship as it. For example, the main goal of computer vision is to extract meaningful information from images or videos whether a certain object is present or not in a particular scene and it is quite complex than others. Similarly, the machine learning is to optimize or enhance differentiable parameters so that a certain cost or loss function is minimized and the goal of image processing is to enhance or compress image or video information at pixel-wise operations.

2.10.1. Digital Image Processing

An image may be defined as a two-dimensional function, f(x, y), where x and y are spatial (plane) coordinates, and the amplitude of at any pair of coordinates (x, y) is called the gray level or intensity of the image at that point. When x, y, and the amplitude values of f are all finite, discrete quantities, it calls the image a digital image [23].

A digital image has different forms and some of them are [24]:

- **Binary image:** This is the simplest form of an image with two gray values, 0 and 1 or black and white. Each pixel is represented by a single bit. These types of images are useful in computer vision applications where only information about images or outlines are required. It can be formed from a gray-scale image that uses 0 for pixels with gray levels lower given threshold value and 1 for other pixels. But this conversion mechanism may create a loss of important information about the image.
- **Gray-scale image:** These images comprise the intensity or brightness information. Represent each pixel by the image’s number of bits. The typical image has 8 bits per pixel which are 256 different possible intensity or gray values from 0 to 255.
- **Color image**: These images are represented as RGB (Red, Green, and Blue), and each pixel has 24 bits which mean 8 bits per zone (RGB).

The field of digital image processing refers to processing digital images by means of a digital computer. Note that a digital image is composed of a finite number of elements, each of which has a particular location and value. These elements are referred to as picture elements, image elements, and pixels. Pixel is the term most widely used to denote the elements of a digital image. Vision is the most advanced of our senses, so it is not surprising that images play the single most important role in human perception. However, unlike humans, who to the visual band of the electromagnetic (EM) spectrum, imaging machines cover almost the entire EM spectrum, ranging from gamma to radio waves. They can operate on images generated by sources that humans are not accustomed to associating with images.

These include ultrasound, electron microscopy, and computer-generated images. Thus, digital image processing encompasses a wide and varied field of applications. There is no universal agreement among authors regarding where image processing stops and other related areas, such as image analysis and computer vision, start. Sometimes a distinction is made by defining image processing as a discipline in which both the input and output of a process are images. This is believable to be a limiting and somewhat artificial boundary [25]. For example, under this definition, even the trivial task of computing the average intensity of an image (which yields a single number) would not be considered an image processing operation. On the other hand, there are fields such as computer vision whose ultimate goal is to use computers to emulate human vision, including learning and being able to make inferences and take actions based on visual inputs. This area itself is a branch of artificial intelligence (AI) whose objective is to emulate human intelligence.

There are no clear-cut boundaries in the continuum from image processing at one end to computer vision at the other. However, one useful paradigm is to consider three types of computerized processes in this continuum: low-, mid-, and high-level processes.

Basically, different image processing applications may follow different steps. However, there are some fundamental steps that every image processing applications pass through as shown in Figure *2.1* [26].

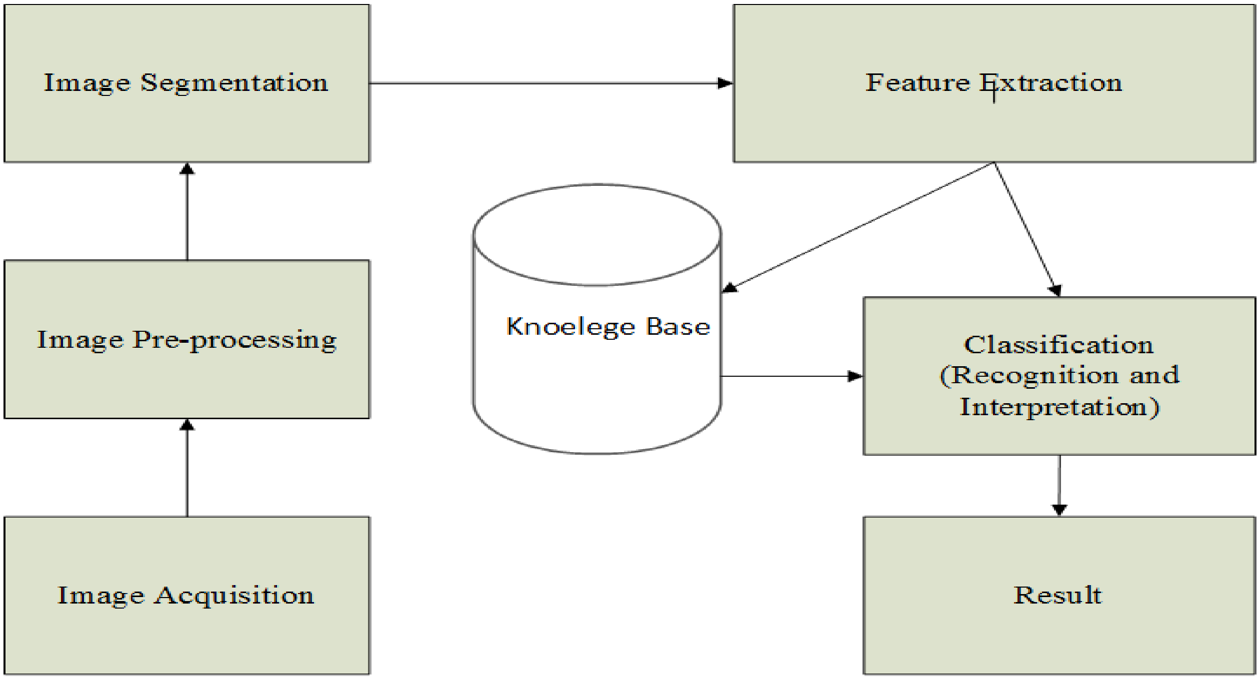

Figure 2.1. Fundamental steps in digital image processing

This subsection promotes image processing by describing the fundamental steps of digital image processing in case of CXR image.

2.10.1.1. Image Acquisition

The image acquisition is the first task or step in any image processing application or system. The general goal of image acquisition is to convert an optical (real world) image into an array of arithmetical data which might be future operated on a computer system before any image or video processing can initiate an image must be captured by the camera and converted into a manageable object [27]. The image acquisition procedure consists of three steps which are the optical system which focuses the energy, then the energy reflected from the object of interest and at the end a sensor which measures the amount of energy. Image acquisition can be achieved by a suitable camera. For example, for an x-ray image use a camera (film) that is sensitive to x-ray, for infrared image use camera which is sensitive to infrared radiation and for normal images use cameras which are sensitive to visual spectrum [28].

The chest radiograph is made for a broad content of signs, including the investigation of respiratory disease, TB, cardiac disease. There are two standard projection methods in order to capture the thoracic image, which is posterior-anterior (PA) and lateral view radiography. The PA is performed standing and in full inspiration and used for better visualization of the anatomy of organs like lungs. The literal view also performed straight left literal and ideal for the confirmation of the presence and location of opacities on frontal X-rays with the combination of PA view.

2.10.1.2. Preprocessing

Once the image is acquired the image preprocessing task will be engaged. Image preprocessing may have dramatic positive effects on the quality of feature extraction and the results of image analysis. Image preprocessing is a combination of corrections and enhancements that are an essential part of a computer vision procedure. The quality of the preprocessing consequently affects the performance of the succeeding processing steps. For TB screening in CXR image, typical preprocessing tasks are contrast enhancement, bone suppression, boundary detection and image transformation. Some of image pre-processing tasks are:

Image Re-sampling

It is the process of transforming a sampled image from one coordinate structure to another i.e. changing the pixel dimension of an image. The re-sampling affects the display dimension of an image. When resampling an image, it can lose some information from the image down-sampling or escalation the number of pixels in the given image, these new pixels are added based on color values of present pixels.

Image Enhancement

Image enhancement is one of the most and simplest motivating areas of digital image processing. Essentially, the idea behind enhancement method is to bring out the fact that is obscured or simply to highlight assured features of attention in an image. For example, increasing the contrast of an image because it looks better.

Image Restoration

Image restoration is an area that also contracts with refining the appearance of an image. Conversely, image restoration is objective unlike enhancement, which is subjective, in the sense that restoration method tends to be founded on probabilistic or mathematical models of image degradation.

2.10.1.3. Segmentation

Segmentation refers to the process of splitting an image into component parts, or into separate objects i.e. sets of pixels. The objective of segmentation is to simplify and/or amendment the representation of an image into somewhat that is more significant and easier to examine. Precisely, image segmentation is the process of conveying a label to each pixel in an image such that pixels with the same label portion certain appearances. The consequence of image segmentation is a set of parts that together cover the complete image or a set of outlines mined from the image.

Segmentation procedures are built on the two basic properties of strength values- discontinuity i.e. partition an image based on sharp changes in intensity and likeness i.e. to partition an image into regions that are similar according to a set of predefined criteria among the pixels. The segmentation should stop when the object of interest in an application has stayed isolated [14].

The Sobel, Robert, Prewitt, Laplacian, and Canny operators are typically used for edge extraction in DIP applications [14] [23]. If the interest is to extract the whole region of an object, a region based method is applied. A region-based approach can use any of a variety of strategies for pixel classification. Threshold-based is also working in several image segmentation process it is based on pixel distribution or intensity based.

Segmentation by Thresholding

Since its spontaneous properties and straightforwardness of operation, image thresholding likes a dominant point in the application of image segmentation. In this technique, the pixels are segregated liable on their intensity value. By choosing a suitable threshold value T, the gray level image can be transformed into a binary image. The binary image should comprise all of the important information around the position and outline of the objects of interest i.e. foreground [29]. So, if an image comprises dissimilar pixel intensities in each region adaptive thresholding picks a separate threshold for each pixel based on the series of intensity values in its resident neighborhood.

2.10.1.4. Feature Extraction

Image analysis includes exploration of the image information for a specific use. Typically, the raw facts of a set of images are examined to gain understanding into what is on with the images and how they can be used to mine intended evidence. In pattern recognition and image processing, feature extraction is a key step, which is a special form of dimensionality lessening. When the input data is too huge to be handled and assumed to be redundant then the data is distorted into a condensed set of feature representations.

The texture of an image region is determined by the way the gray levels are distributed over the pixels in the region. Although there is no clear definition of "texture" in literature, often it describes an image looks by homogeneous or inhomogeneous, irregular or smooth, fine or rough, etc. The features are described to quantify properties of an image region by exploiting space relations underlying the gray-level distribution of a given image. The process of transforming the input data into a set of features is called feature extraction. Features frequently contain evidence relative to shape, color, context or texture.

Many methods have existed used to extract features from images. Some of the regularly used methods are like: spatial, transform features, edge and boundary, color, shape and texture features.

2.10.1.5. Classification

Classification contains a broad range of decision theoretical methods to the identification of images [14]. All classification procedures are based on the assumption that the image in question shows one or more features and that each of these features goes to one of several separate and exclusive classes. The classes may be specified by an analyst (as in supervised classification) or automatically clustered (i.e. as in unsupervised classification) into sets of prototype classes, where the analyst merely specifies the number of desired categories.

The classification algorithms consist of two stages of processing: training and testing. In the initial training phase, characteristic properties of typical image features are isolated and, based on these, unique description of each classification category, i.e. training class, is created. In the subsequent testing phase, these feature-space partitions are used to classify image features.

Several classifiers have been described for the computerized recognition such as Bayes classifier and different types of Artificial Neural Networks (ANNs), local linear map, SVM, k-mean and fuzzy system has been extensively used as a classifier for several recognitions and detections [30] [24].

2.10.2. Machine Learning

In order to formulate and implement the intended model from this thesis, know-how about machine learning is important. Machine learning is a branch of AI that employs a variety of probabilistic, statistical and optimization methods that allow computers to learn from past patterns or practice and to use that prior training to categorize new data, identify new patterns or predict fresh trends [31]. Machine learning has been the subject of great interest in the biomedical environment because it deals promise for refining the sensitivity and/or specificity of finding and diagnosis of disease. Recently, given the dramatic growth in medical data being collected, novel diagnostic modalities being settled and the complexity of the data types and importance of multimodal investigation the need for an automated system is better than ever.

Traditionally used machine learning algorithms range from simple, probabilistic classifiers like Naïve Bayes [32], which once learned from existing data, classifies a new data instance by calculating the posterior probabilities of a hypothesis to more complex algorithms like Neural Networks that loosely simulate information processing by human brain, and that involve feed-forward and error propagation algorithms [31]. Reinforcement learning is alike to usual supervised learning if the problem includes just two classes and equal cost of error [32].

2.11. RELATED WORKS

2.11.1. Overview

For the purpose of conducting this research, the development of the state-of-the-art current knowledge regarding methods that researchers were followed during their study work is a very essential task and initial point of the entire work. Based on the article’s primary intention among image processing stages in CXR image the analysis is organized into three themes: the segmentation, the feature extraction, and the overall TB screening using CADe.

In the next consecutive subsections, the important points like objective(s) settled, problem(s) stated, the methods followed, key-points, the result obtained, and the open issues from each article are identified and included under perspective themes such as Segmentation, Feature Extraction and a general CADe in CXR image. Finally, the correlation of all reviewed articles and the open issues can be addressed whether or not by this study also summarized.

2.11.2. Segmentation

In this section, the relevant articles related to the lung segmentation in CXR image are reviewed. Due to this two articles were considered and highlighted accordingly as stated below.

Karargyris A. etal. [33], built a system that can bring about population screening in resource-limited areas wherein the use of CXR image by improving their previous similar work [34] by joining texture and shape features of the image to notice pulmonary anomalies. In order to accomplish the objective which is to build a TB screening system and improve their previous contribution, the researchers were identified three main agendas: ***a)*** difficulty of tasks to construct a robust automated application used to detect TB and still it is an open research area, ***b)*** the variability of image quality, size, shape, and texture of CXR image, ***c)*** texture information is not sufficient to screen and geometrical shape information is needed especially for classification that used to acquire overall performance.

Based on the above limitation, the researchers have formulated three assumptions as a research hypothesis: i.e. *Assumption-1* (adjusting the segmentation unit to track the structure of lungs i.e. red outlined in Figure *2.2*. and (a) incorporate the segmentation behavior of the two experts shown. (b) As a substitute for air cavities and the intervention of radiologist as an observer is needed). *Assumption-2* (geometric changes between lung fields by adapting the algorithm to comprise the notion of relative diagnosis) and *Assumption-3* (accumulation CXR models of TB cases by accumulation binary masks of abnormal CXRs).

Aside from the above assumptions, air cavity and lung anatomy segmentation techniques were examined and air cavity segmentation method performed better than lung anatomy segmentation in almost all parameters for the first two assumptions when combining the texture and shape features. Accumulation binary masks of abnormal CXR took from JSRT dataset has been performed better performance the overall segmentation process for the third assumption.

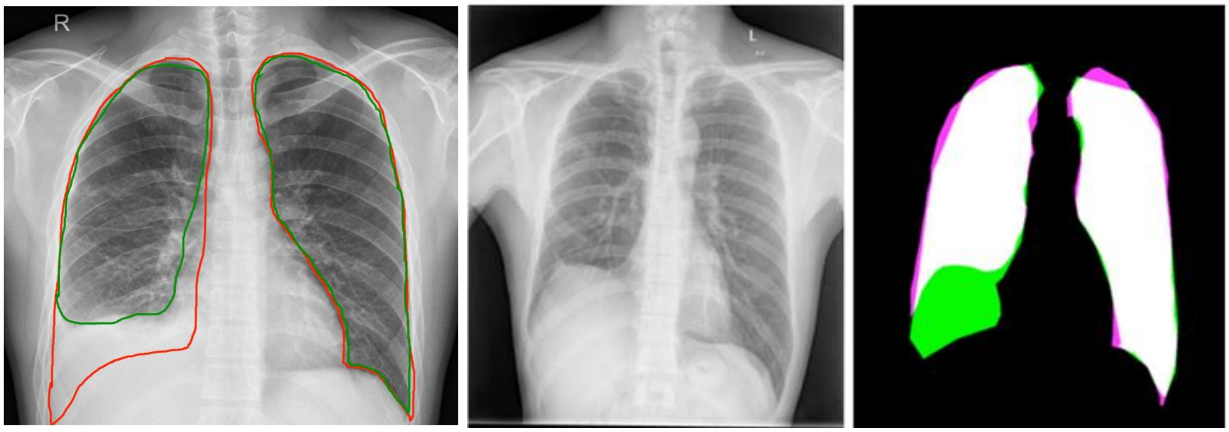

(a) (b)

Figure 2.2. Two different segmentation methods proposed

The Figure *2.2* shown above, the expected lung anatomy segmentation colored in red and air cavity segmentation also colored in green and labeled by (a), the Right: radiologists' markings, the left also: abnormal cases, (green: reviewer A, purple: reviewer B, white: overlapping zone between reviewer is labeled by (b).

Alike, Kiran M. etal. [35], proposed a flexible lung segmentation techniques called Sauvola thresholding-Gaussian derivatives in CXR image. The technique is used four Gaussian derivatives responses. As reported, using Sauvola image thresholding which typically places of interest the inner area of the lung region. To highlight the lung region completely the Sauvola threshold image and gradient average image is combined then remove the noisy area such as the trachea, clavicle region and outer body, XOR is applied between similar CXR average image and combined image are basic tasks. The proposed solution was tested on the two public datasets JSRT, Montgomery, and one private set and achieved 94.57%, 90.75%, and 65.25% accuracy respectively using the Jaccard coefficient.

2.11.3. Feature Extraction

In this category, how researchers have extracted lung features from CXR image for the purpose of TB detection are examined with two selected articles outlined below.

Singh N. etal. [36], implemented an approach for lung's feature extraction methodology from CXR image for TB detection, the study also examined the two pertinent image descriptors which are shape and texture using different descriptors and the Gray-Level Co-occurrence Matrix (GLCM) followed by the log Gabor filtering techniques. Finally, by applying SVM classifier, the ROC curve and confusion matrix of classifier shown an AUC of 0.98 and 0.96 on MC and Schengen dataset, respectively, with 100% specificity. But, limited instances were considered from the two datasets.

Likewise, Szilard V. etal. [37], established a feature extraction methodology to find the optimum feature set from a greater pool of common image features, which is used originally for problems such as object recognition, image retrieval, etc. they used about seven different shape and texture descriptors like: Intensity Histogram, Gradient Magnitude Histogram, Shape Descriptor Histogram, etc. For performance assessment measures such as AUC and ACC were considered. Using a CNN classifier on two publicly available data collections, MC and the Shenzhen dataset, they achieved the AUC and ACC of 0.99 and 97.03%, respectively.

2.11.4. TB Screening using CADe

In this subsection, the general TB detection or screening mechanisms in CXR are examined. For this knowledge development, three relevant articles are outlined below.

Rajaraman, S. etal. [38], attained TB detection models in CXR image. The study was proposed two different proposals such as feature extraction using local and global feature descriptors and classification using SVM, and feature extraction using pre-trained CNNs and classification using SVM. The study was used four different datasets from different territories including the two public CXR datasets. For Proposal 1, the images were down sampled to 4096×4096, 3072×3072, 2048×2048, and 1024×1024 pixel. For Proposal 2, the images were down sampled to 227×227 and 224×224 pixel resolutions to suit the input necessities for the different pre-trained CNNs, across all the datasets. Based on their investigation, the second proposal was more effective than the first one by minimizing the computational time accuracy.

Similarly, Jaeger S. [39], developed a new methodology for the purpose of implementing a timely diagnosis of drug-resistant TB. For the development, about 135 instance dataset was used aside patients' day to day follow-up as patient history attachment. Thus, the solution attained AUC >66% performance.

Table 2.3. Summary of related works

Citation	Author	Title	Performance	Dataset	Open Issue
[33]	Karargyris A. etal.	Combination of texture and shape features to detect pulmonary abnormalities in digital chest X-rays	AUC 85.4%	Shenzhen and JSRT datasets	Manual segmentation made by Experts
[35]	Kiran M. etal.	Chest X-ray segmentation using Sauvola thresholding and Gaussian derivatives responses	AUC 94.57%, 90.75%, and 65.25% on three different datasets	JSRT, MC, and one private set	Not attractive because of overlapping with other organs like trachea the obvious case
[36]	Singh N. etal.	Tuberculosis Detection Using Shape and Texture Features of Chest X-Rays	AUC of 0.98 and 0.96 on MC and Schengen dataset	Part of MC and Schengen dataset	Selected images, they may ignore low quality images. Because standard datasets are prepared intentionally by adding images with different defects by expertise.
[37]	Szilard V. etal.	Feature selection for automatic tuberculosis	AUC and ACC of 0.99 and	MC and Schengen dataset	Applied lung model for best fitting for the segmentation task,

		screening in frontal chest radiographs	97.03%, respectively		thus, the performance depends on the lung model
[38]	Rajaraman S. etal.	A novel stacked generalization of models for improved TB detection in chest radiographs	Variable	JSRT, Montgomery and others two from Kenya and India a total of 2073	Used manual boundary box in order to get ROI and this may not effective an image with an improper acquisition.
[39]	Jaeger S. etal.	Detecting drug-resistant (DR) tuberculosis in chest radiographs	AUC up to 66% among drug-resistant cases	The 135 cases consist of 45% sensitive (61) and 54% DR (74) cases	Too low performance even if supported by patient history. Small dataset and limited coverage or location.

In this subsection, about six most relevant articles to the proposed model were reviewed by categorizing based on their nature and intention of the proposed study such as segmentation, feature extraction and the overall CADe system. Paralleled with the review, the open issues on each article to be addressed by this study and/or identify them as future work are identified in Table ***2.3***. Thus, most of the articles used public datasets, especially MC and Schengen dataset and almost all of them are used at least lung model or the radiologist support to identify ROI object from the image. Some of the articles are also used limited or selected images among the dataset for the implementation and such limitation defect the overall performance of the study.

As part of this study, the study is proposed a new approach i.e. a TB detection model without any interferences neither expert support nor the predefined lung model like lung mask that the mask constructed or outlined by experts due to extend. Plus to this, the proposed model is implemented on three public datasets by considering all instances gives about a total of 1047 instances. Consider all instances in the model is used to increase model tolerance because the datasets are prepared by experts intentionally with variety of image profile i.e. high or low quality, age diversity or patient's body size. Beside the imaging model, the overall performance of diagnosis method can be extended by comprising patient's medical history but such dependent inputs are not considered in this proposed model due to the aim of the study.

2.12. Conclusion

In order to formulate the relationships between the actual problem foundations i.e. early detection of TB and the solution approach also supporting the diagnosis mechanism using DIP discipline with the help of machine learning this chapter plays a great role. To examine benchmarks and limit the re-wheeling already solved by researchers as a current solution is also stated in this chapter in different subsections general to specific.

In this chapter, the current state-of-the-art about TB detection in CXR imaging modal is formulated. The segmentation, feature extraction and overall TB screening methodologies are examined. Based on the identified open issues from each major articles, the proposed model was considered other researchers' gap. In the next chapter, the entire methodological approaches of the proposed solution are identified.

CHAPTER THREE

3. MATERIALS AND MOTHODS

3.1. Introduction

From the establishment and answering the study's questions as mentioned in subsection 1.3, the methodology involves thorough procedures, which is a route and roadmap that ranges from problem formulation to evaluation. Similarly, to accomplish the proposed study, the methodology directly represent the way how goes the proposed solution. Thus, the design science approach is taken for the accomplishment of the proposed solution. The design science approach is a solution- oriented approach [40] and it is the design and investigation of artifacts in context, unlike other natural and social science research methodologies those are problem-oriented. The basics of this proposed model is the current state-of-the-art in the research area and the intention of the study is adding innovative solution on the current context. Thus, for this proposed model a new and innovative research standard i.e. design science is accepted.

Through this, the chapter consists of the ways of realizing the research question and objective in subsection 3.2, the formulation of the-state-of-art of the problem and need of the advancement in the area as mentioned in subsection 1.3 through the literature review as shown in subsection 3.3, the description of required and selected datasets by the proposed solution in subsection 3.4, the design and implementation procedures of the proposed solution in subsection 3.5 and also the validation and performance evaluation techniques in subsection 0 is stated.

3.2. Defining Problem and Objective of the Study

In order to define a specific research problem and justifying the worth of a solution, problem understanding and rationalization has been taken out in the proposal phase, especially, in the first four main topics of chapter 1. In this study, the lack of automatic segmentation of lung area in CXR image and feature extraction methodology in another aspect of the study are considered. The foundation to carry out this research work and means required by this study, the objective of the study is given in subsection 1.4.

3.3. Literature Review

In order to identify the stakeholders, goals, phenomena, evaluation, diagnosis, representation of knowledge questions, causes, mechanisms and reasons the systematic extraction of knowledge from the existing literature is the crucial task. Thus, a literature survey was conducted on the area of image processing for every stage of the system. Available journals, books, case studies, previous research works & guidelines were analyzed.

During the analysis, the snowball methodology system which is article searching and analyzing strategy starting from research area to specific or single article in the field was followed with the help of the two key-phrases (TB screening in CXR image) and (TB feature extraction and classification in CXR image). Then, about six relevant articles were selected for this knowledge creation stage and gap analysis. Among the literatures many of them were applied almost all image processing cycles (starting from pre-processing to classification) but some of them were considered two or more processing steps. The steps carried out the literature analysis is shown below.

3.3.1. Defining Search Questions

In order to observe overview of research area, identify the quantity of research to be reviewed on and result existing within it, the following enquiries are identified:

- Which journal databases include papers on TB detection in CXR Image?
- What are the most examined topics written on TB detection in CXR Image?

3.3.2. Source of Literature

To extract relevant reference, reference databases were explored with customized search string followed by manual filtering of the result and using predefined inclusion and exclusion criteria. To search relevant papers on TB detection or diagnosis in CXR image, the following five reference databases were used.

1. IEE Xplore
2. Google scholar
3. SienceDirect
4. Springer

5. Elsevier

With the specified reference databases, search for a paper between the time period 1st of Jan 2012 and 11st of June 2019 was applied. Chosen 2012 as a starting date because the work published on specified year was referenced by another core related work and 11st of June 2019 was the last date of searching for the literature.

3.3.3. Screening Process

Papers are filtered using inclusion and exclusion criteria. Whenever paper meets all inclusion criteria, it was kept for further considerations and when the paper meet exclusion criteria, it was removed from the study.

Inclusion criteria: research work within focus area of TB detection in CXR image. The research work must address the TB, CXR image and image processing.

Exclusion criteria: articles written in the non-English language, topics of similar words with TB but not in computer science and engineering concept (for instance TB in from environmental or medical diagnosis aspect unlike in CXR), and papers published before 1st of Jan 2012 and after 11st of June 2019 in terms of the base paper for the first related work article and the final date for the thesis documentation respectively.

Using the recommended reference databases listed above, the actual reference instances were shown in Table *3.1* with both technical search keys mentioned above. Then, the research papers were filtered by reading the abstraction and introduction section of each paper. Finally, 27 references are selected based on their relevance to the proposed model with the two keys i.e. key-1 and key-2 and phrases TB screening in CXR image and TB feature extraction and classification in CXR image respectively.

Table 3.1. Article searching process from the reference databases

Reference database	Primary instances		Merge and filter		Selected	
	Key-1	Key-2	Key-1	Key-2	Key-1	Key-2
1. IEE Xplore	12,768	7,861	32	14	3	2
2. Google scholar	18,100	13,562	67	53	4	4

3. SienceDirect	247	567	13	17	2	3
4. Springer	15678	11,967	34	43	2	1
5. Elsevier	5577	7635	21	34	1	2

3.3.4. Extraction Method

While keeping the research questions and the source identification questions in mind, the distilled of the results regarding the extracted references and the content of the researches were supplemented.

3.4. Dataset

Most of the articles studied in the area were implemented and evaluated on publicly available datasets. In order to evaluate the study with other studies using similar dataset is needed. Therefore, the study was evaluated on three CXR datasets including two publicly available datasets provided by the U.S. National Library of Medicine (NLM), National Institutes of Health (NIH) described in [13], i.e. Shenzhen and Montgomery Country (MC). The third dataset was Japanese society of radiological technology (JSRT). The summary of each dataset is presented in Table *3.2* below.

Table 3.2. Summary of Datasets

No	Name of the Dataset	No of Images	No of Infected Images	No of No-infected Images	Resolution (in pixels)	Grayscale Level	Image Format
1	Montgomery Country (MC)	138	58	80	4020 × 4892 or 4892 x 4020	12-bits	PNG
2	JSRT	247	154	93	Fixed size 2048 × 2048	12-bit	IMG
3	Shenzhen	662	336	326	approximately 3000 × 3000	12-bit	PNG
	Total	1047	548	499			

3.5. Solution Design

In this study, the artifact is a DIP model where research contribution is embedded. To create the model, its desire functionality is determined from related work i.e. it extends the knowledge base or applies existing knowledge in new ways. Thus, the contribution of this phase and the research work is an automatic TB detection model in CXR image, and therefore, this enables the alternatives way of diagnosis the TB by radiologist.

In such a process, first, prepare the dataset including format conversion from IMG to PNG file in JSRT dataset, scaling or normalizing the image resolution, make the input CXR image to borderless form are major image preprocessing task which is considered by this proposed model. Second, the detection of ROI is another task then segment detected image from the original image. Third, extract textural features which determine the image with its individual profile. Finally, the classification of the extracted features as an input using classifier. The proposed model is discussed in chapter 4.

3.6. Implementation

The proposed model implements and then demonstrates the instance of the solution. As such, the demonstration mainly concerned with the use of the proposed model for, specifically, implement step by step of model demonstration starting from data preparation to validation then the performance evaluation. The implementation of proposed model described in chapter 5.

3.7. Validation and Performance Evaluation

In order to evaluate the performance of proposed system, by obtaining the extracted textural features from each dataset, the solution was validated using 10-folding validation technique acquired by Matlab classification learner toolbox. To evaluate the overall performance of the proposed solution, the three performance metrics ware conducted such as: explicitly Specificity (SPC), Sensitivity (SES) and Accuracy (ACC):

3.8. Development Tools

The proposed model i.e. to detect lung TB in CXR image is implemented using the following tools and materials.

Table 3.3.Development tools and materials

Type of tool or material	List	Description or Specification	Purpose
Programming Language	Matlab	Version 2018a	To implement the entire proposed solution (from dataset preparation and preprocessing to evaluation of the proposed model)
Development Libraries	Matlab Machine learning toolbox	Classification learner module	To train the machine and evaluate the model

Experimental setup	Laptop	**Processor:** Intel(R) Core(TM) i7-47MQ CPU @ 2.40GHz 2.40 GHz	To conduct the overall experimental processes
		RAM: 8.00 GB	
		System Type: x64-based processor and x64-bit Operating System(Windows 10)	
		HDD: 2TB	

CHAPTER FOUR

4. PROPOSED MODEL

4.1. Introduction

In this thesis, a model for automatic lung TB detection in CXR is proposed. Basically, the proposed framework has five main modules: image preprocessing, detection of lung region, the segmentation, feature extraction and classification.

In this chapter, the detail processes for the preprocessing, detection of lung area, the segmentation of detected area and textural feature extraction of the proposed model is presented.

This chapter is structured as follows. Section *4.2* reflects about the overall proposed model. In section *4.3*, the aspects of dataset preparation is planned. Section *4.4* describes the image preprocessing manners of the proposed model. Section *4.5* describes the process used to initially detect the area of lung area from a given CXR image in the proposed model that consist of image transformation and repetition of same task until to get relatively an accurate fit. In section *4.6*, the segmentation of detected area of lung boundary is described. And also section *4.7* and *4.8* elaborates the extraction of textural features extraction using first-order and second order or GLCM and the classification of the proposed model respectively. Finally, section *4.9* describes the performance evaluation techniques are given accordingly.

4.2. Proposed model

The typical image processing steps are working in any image processing application environments. Unlike the normal image acquisition mechanism like photo camera, medical imaging is very tedious task and the image will be overlapped by different human organs. Thus, the image processing task in medical image processing is more challenging.

Based on the thesis aim i.e. TB detection model in CXR image, all DIP stages are accumulated as shown in Figure *4.1* below.

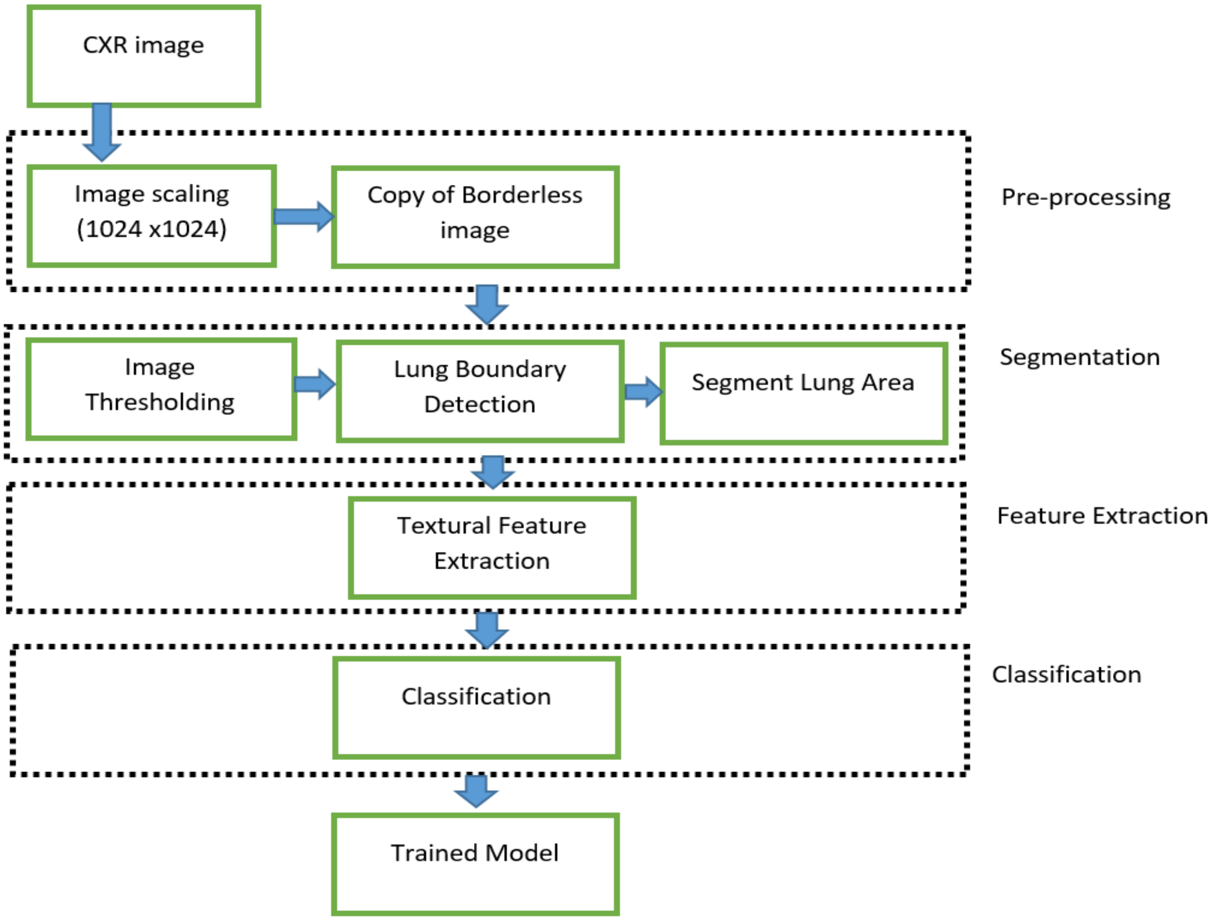

Figure 4.1. A block diagram for the proposed model

4.3. Dataset Preparation

To train and test the proposed model, a total of 1047 images are collected from three public CXR datasets as shown in previous chapter section *3.4*, among these 548 images are abnormal and the remaining 499 images are also normal. All images collected from the three datasets are considered as study's train and test dataset. In one of the datasets i.e. JSRT set, the images are in IMG format, due to this the images should be converted to one of the portable image format i.e. PNG which is a common image format for the others two datasets. Ordinarily, the converted image is positioned in back to 270 degree position and in mirror direction that needed position adjustment or rotation and image flipping respectively. The detail implementation of the dataset preparation is shown in Algorithm *4.1* below.

Input - JSRT IMG or binary data

Output – converted image from IMG to PNG format using the Matlab functions

Calculate number of binary data D in JSRT dataset;

For each IMG image i in D

locate the file i;

open the binary data i from the local drive using fopen function;

slice the binary data with 2048 x2048 matrix;

convert the sliced a matrix data to gray level using mat2gray function;

rotate the default position to normal using imrotate function with 270 position;

convert the rotated image from mirrored to unmirrored direction using flip function;

store the processed gray image to the local drive using imwrite function;

End

Algorithm 4.1. The conversion step from JSRT binary data to image format

4.4. Preprocessing

Each dataset has different resolution, even if under the same dataset the resolutions between images are different. Therefore, image normalization should be attained. The preprocessing section does basic and intensive tasks such as image scaling from variable resolution to one uniform size as mentioned in Algorithm *4.2*, removing nonzero pixels which are connected with the border. In most articles, the normalization task shown that the image normalization is to low up to 224 x 224 to attain best performance during implementation, especially, in medical image analysis [38]. But, if the work is on the statistical feature, too low resolution or size is not effective. Thus, to achieve the intended result from this study the images are normalized to the average resolution i.e. 1024 x 1024 image resolution.

Input – un-normalized image←different and/or big size

Output – normalized (1024 x1024) image

Calculate number of image D in the dataset;

For each image i in D

locate the file i;

open the image i from the local drive using imread function;

resize the image i with 1024 x 1024 resolution using imresize function;

store the processed gray image to the local drive using imwrite function;

End

Algorithm 4.2. Normalizing the image size

Segmentation of CXR images has several challenges such as the distortion produced by the medical or personal equipment, poor contrast, diverse size of lungs and basic shape varieties due to an infection or age as shown in Figure *4.2*.

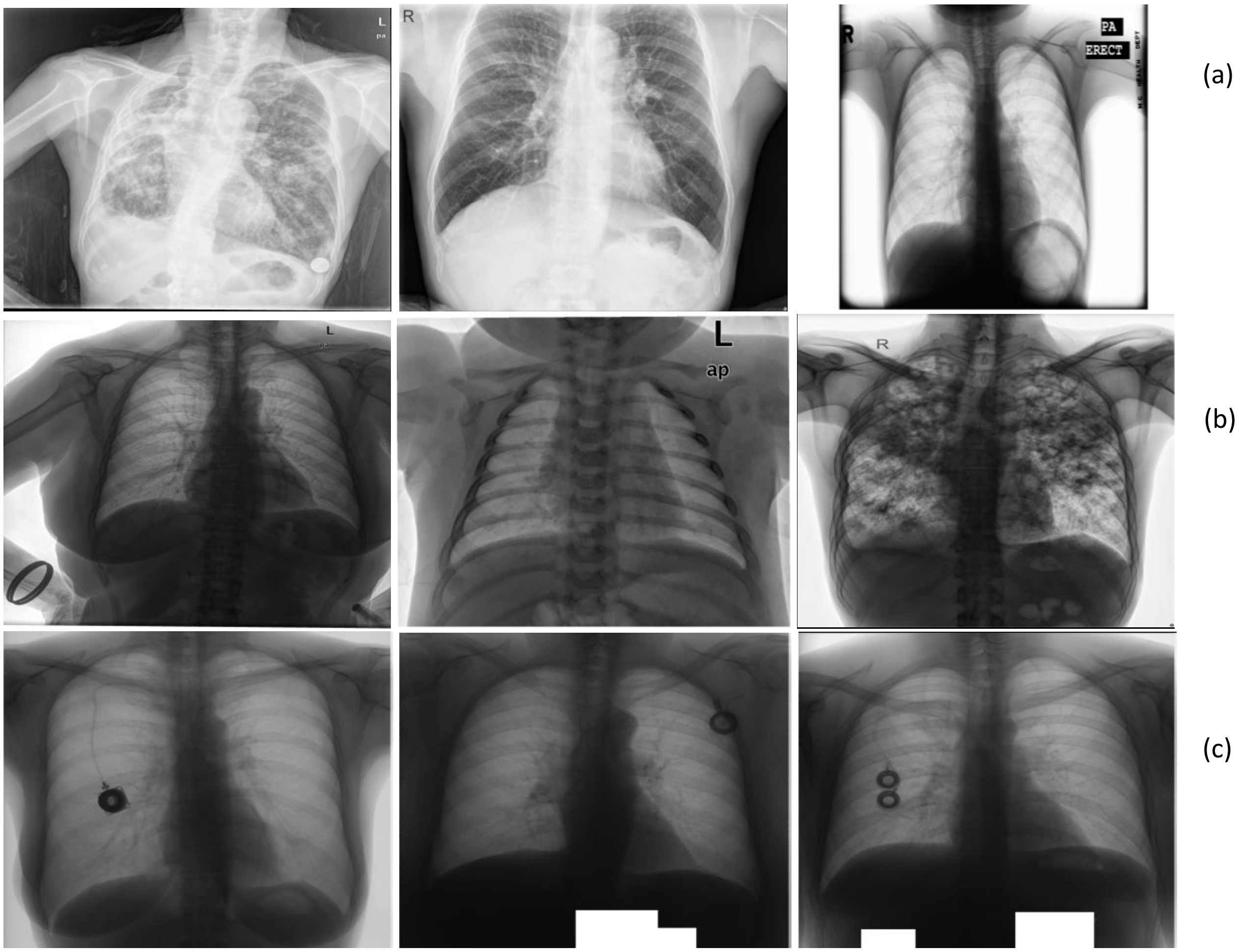

Figure 4.2. Some distorted images from the datasets

The graphical view of some of the challenges is shown in Figure 4.2, labeled as (a), (b) and (c) that are sampled from MC, Shenzhen and JSRT dataset respectively.

Usually, the input CXR image contains both foreground i.e. lung region and background information. To remove the background information that is lighter than the neighboring from a given image, researchers were proposed several solutions. But, using gray-level image the extraction of the foreground information is challenging unlike RGB image due to limited pixel value range between 0 and 255 both inclusive. In CXR image most of the background information are connected to the border and the acquisition technique also in gray-level.

Input – 1024 x1024 gray-level CXR image ← the gray-level is the default color depth in ← the datasets	
Output – 1024 x 1024 borderless image which contains lung objects (left and right)	

Calculate number of image D in the dataset;

For each image i in D

locate the file i;

open the image i from the local drive using imread function;

remove non-zero intensity values from the image i using Matlab imclearborder function-with 4 connectivity;

store the processed image to the local drive using imwrite function;

End

Algorithm 4.3. Clear image border

In this proposed model, the clear border algorithm [41] is applied that to remove background information from the CXR image. This algorithm is used to remove the structures that are brighter or non-zero pixel values which are associated with the image border as shown in Algorithm *4.3*. Due to its implementation, using Matlab image processing toolbox, the input can be either binary or gray-level image then the output is binary or gray-level image respectively. To make the removal of information from the image, there are two possible connectivity in 2d image i.e. 4 or 8 and the default is 8, but in 3d image 6, 18 and 26 are possible connectivity and the default is 26. In this study, the images are in 2 dimension and the 4 connectivity is applied for optimum computational time than 8 connectivity.

The process of extracting the lung objects from CXR image, image thresholding methods were applied using both global i.e. Otsu thresholding [29] [42] and local thresholding methods independently, then after, the result with best fitting is used for further implementation processes as an input as shown in Algorithm *4.4*.

Input – 1024 x1024 borderless gray-level CXR image

Output –three independent binary images with two lung objects inside 1024 x 1024 image

```
Calculate number of image D in the dataset;
For each image i in D
    m=i; ←Copy image i into m to calculate the second threshold method
    n=i; ← Copy image i into n to calculate the third Otsu threshold method
    For  each j in 1024
       For each k in 1024
         If (i[j][k]>0.01)    ← method 1, the threshold value 0.01 proposed by this study
            i[j][k]=1;
         Else
            i[j][k]=0;
         End
         If (m[j][k]>0.001)  ← method 2, the threshold value 0.001 proposed by this study
            m[j][k]=1;
         Else
            m[j][k]=0;
         End
      End
    End
    n=imbinarize(n, 'adaptive'); ← method 3, the Otsu threshold method
    store the three images to the local drive using imwrite function individually;
End
```

Algorithm 4.4. Object detection by applying three different threshold values

In the study, the preprocessing tasks continued to acquire and fill the holes which are surrounded by the two selected lung objects.

4.5. Detection of Lung Region

At this level the majority of the preprocessing tasks are over and the approximate lung area is detected. Furthermore, in order to sharpen the lung objects (left and right side lungs) from CXR image, object sharpening algorithms are needed which includes dilation and erosion [43]. Using Matlab image processing toolbox, the built-in functions imdilate, and imerode are taken for the object sharpening as shown in Algorithm *4.5* below.

Input –binary image from one of the three selected threshold outputs

Output – the sharpened lung objects in image

Calculate number of image D in the dataset;

For each image i in D

  locate the file i;

  open the image i from the local drive using imread function;

  filter the two lung objects in i using Matlab bwareafilt function;

  fill the area surrounded by the two lung objects in i using Matlab imfill function;

  sharpen the fragmented edge of the lung objects in i using imdilate and imerode function;

  store the processed image to the local drive using imwrite function;

End

Algorithm 4.5. The lung objects sharpening

4.6. Segmentation

In segmentation technique the texture feature parameter is an image analysis technique in the field of computer vision. In CXR, it is difficult to isolate the lung fields using pure pixel-based approaches. In the segmentation field, there are many techniques that used to segment the images.

In the above scenarios, the relative location of the lung objects in image can be located. Here, the actual lung area is detected using the overlapping technique i.e. Exclusive OR (XOR) to extract the lung area from the background and the algorithm used is depicted in below.

Input – the sharpened lung objects in CXR image

Output – segmented lung objects from the original CXR image

```
Calculate number of image D in the dataset;
Calculate columns c and rows r in image
For each image i in D
    locate the file i;
    open the original image i from the local drive using imread function;
    open the sharpened lung objects image j from the local drive using imread function;
    calculate columns c and rows r in image i;←variable c and r are common for both i and j
    For reach  m in r
        For each n in c
            If (j[m][n]=0)
                i[m][n]=0;
            End
        End
    End
    store the processed image i to the local drive using imwrite function;
End
```

Algorithm 4.6. The lung object segmentation

4.7. Textural Feature Extraction

The textural profile of the normal and abnormal images are relatively different in depth of their gray-level. Especially in CXR images, i.e. the abnormality can be expressed by depth of the actual color than the normal one, because, parts of the organs could be affected by the infections like lung TB in lung organ. In this proposed model, the texture of a segmented region is analyzed using different statistical methods which are a combination of first-order and second-order textural features extraction parameters.

Texture analysis methods can be categorized into statistical, structural, transform and model-based. The effect of basic statistical methods clues to high representations of textures in an image and the gray-level histogram labels the texture of an image. The proposed model adapted the textural feature analysis techniques with ten parameters which are the first five from the first-order and another five also from the grey level co-occurrence matrix (GLCM) features extraction parameters applied as described below.

4.7.1. Grey Level Co-Occurrence Matrix (GLCM)

The statistical technique of considering the texture of an image is that it reflects pixel phenomenon relationship with grey level. The GCLM was primarily proposed [44] with four second-order parameters such as contrast, energy, correlation and entropy then the GLCM also enriched [10] by adding extra feature extraction up to 22 parameters. This GCLM technique also adapted in many technical procedures starting from image segmentation to textural feature analysis [45] [46] [30]. The texture features using GLCM are determined by seeing the rate of pixel pairs with the values which agrees on the grey level in spatial connection of an image and extracting the factors from the matrix [47]. In this subsection, the major and primary GLCM parameters with their brief scenarios are discussed accordingly.

1) Energy

Here, the texture features are determined from the energy events and the high value of energy parameter specifies the grey levels remain constant or periodic. The energy parameter of an image can be characterized as:

$$\text{Energy} = \sum_{i=1}^{n}\sum_{j=1}^{n}(GLCM(i,j)^2)$$

Equation 4.1. Mathematical representation of Energy

2) Contrast

Contrast can be examined based on rough texture in an image and high rate of contrast is obtainable in rough texture. The contrast in expressions of grey level specifies the large dissimilarity of the grey level in an image [48]. The contrast parameter of an image can be characterized as:

$$\text{Contrast } = \sum_{i=1}^{n}\sum_{j=1}^{n}(i-j)^2\big(GLCM(i,j)\big)$$

Equation 4.2. Mathematical representation of Contrast

3) Homogeneity

In an image the homogeneity events specify the homogeneity situation of a pixel. The influence of rise in homogeneity dealings specifies the similar grouping of pixel pairs [48]. The homogeneity parameter of an image can be characterized as:

$$\text{Homogeneity } = \sum_{i=1}^{n}\sum_{j=1}^{n}\frac{\big(GLCM(i,j)\big)^2}{1+(i-j)^2}$$

Equation 4.3. Mathematical representation of Homogeneity

4) Entropy

The parameter entropy in an image defines the degree of the inverse of homogeneity or non-homogeneity of pixel pair in the image. The GLCM provides large values of entropy then to get the constant texture character the entropy is reflected small. The entropy parameter of an image also can be characterized as follows:

$$\text{Entropy } = \sum_{i=1}^{n}\sum_{j=1}^{n}GLCM(i.j)x\log(GLCM(i.j))$$

Equation 4.4. Mathematical representation of Entropy

5) Correlation

The grey level parameters on adjacent pixels determine the correlation texture of an image. The correlation of an image is specified as:

$$\text{Correlation } = \sum_{i=1}^{n}\sum_{j=1}^{n}\frac{(ij)(GLCM(i,j)-\mu_1'\mu_2')}{\sigma_i'\sigma_j^{j'}}$$

Equation 4.5. Mathematical representation of Correlation

As proposed on consecutive articles [44] [10] on textural feature extraction methods i.e. GLCM, beside the above five (#5) main parameters of GLCM, this study considered and used the seventeen (#17) GLCM parameters namely the contrast, correlation, cluster prominence, cluster shade, difference-entropy, difference-variance, dissimilarity, energy, entropy, homogeneity, maximum probability, information measure of correlation, sum average, sum entropy, sum of squares, variance and sum variance. Hence, parameters except the main are second-order parameters that are taken based on the main parameters of the GLCM.

4.8. Classification

The aim of this study is to distinguish the lung area is infected by TB or not in CXR image i.e. need to acquire two classes which are infected and non-infected case. Among classifiers which are reported by researchers [49], the Support Vector Machine (SVM) [50] which is restricted to consider two-classes is selected. SVM, which is a supervised learning algorithm, is used as a classifier in this study to detect CXR with TB manifestations.

In order to evaluate the performance of the proposed model, the dataset should be segmented in to two subsets namely train and test sets. Using cross-validation [51], the k-folds technique was used i.e. 10-folds, because each instance has a chance to consider as in test and train set on different occasion. In the case of 10-folds dataset clustering i.e. train and test set, there is no defined bridge between sets. But, the dataset will grouped in to two that are 90% and 10% for train and test set respectively and the training and testing operations will be executed for 10 times repeatedly. In this case, each test group will be considered as test group for one testing operation only but in 9 training operations.

4.9. Performance Evaluation

To evaluate the overall performance of the proposed solution, the following three performance metrics are conducted, explicitly Specificity (SPC), Sensitivity (SES) and Accuracy (ACC):

$$SES = \frac{\text{True-Positive}}{\text{True-Positive + False-Negative}}$$

Equation 4.6. A mathematical formula for sensitivity

$$SPC = \frac{\text{True-Negative}}{\text{True-Negative + False-Positive}}$$

Equation 4.7. A mathematical formula for specificity

$$ACC = \frac{\text{True-Positive + True-Negative}}{\text{True-Positive + True-Negative + False-Negative False-Positive}}$$

Equation 4.8. A mathematical formula for accuracy

4.10. Conclusion

The chapter was focused on the detail explanation about the processes that are considered by the proposed model. The next chapter also stated the implementation of the proposed model with appropriate illustrations.

CHAPTER FIVE

5. IMPLEMENTATION

5.1. Overview

Based on the specified propped model in chapter *4*, from this chapter, expected to show step by step implementation events of the proposed model staring from the image preprocessing task to evaluation of the model. As mentioned in the proposed model, each step has its own separate sub processes and in, process and out sessions. Therefore, in this chapter, the implementation of the proposed model at each basic image processing steps is shown how and what look like. During the scenario presentation below, each step was demonstrated with a single image and it works for all images i.e. 1047 images in the dataset.

5.2. Dataset Preparation

Among the datasets, the third dataset i.e. JSRT is cannot be accessed directly in Matlab unlike others two. Because, the dataset or each image was formatted with IMG type. Due to this, the image slicing task was done and used PNG image format with an appropriate resolution (2048 x 2048) the detail Matlab code is shown in Appendix: *A*. The process was yielded as shown in Figure *5.1* below that the sliced, rotated but mirrored and un-mirrored images labeled as (a), (b) and (c) respectively.

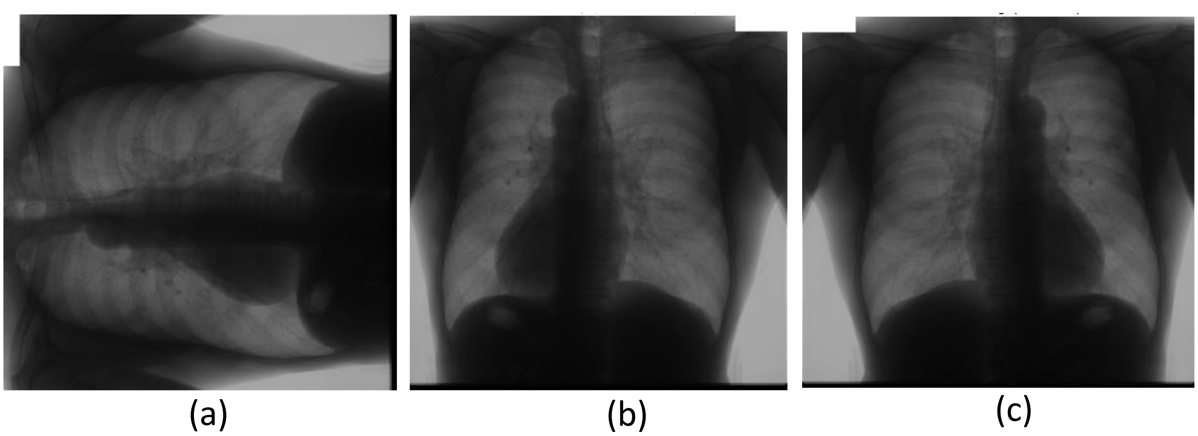

Figure 5.1. Slicing image in JSRT dataset

The intensity profile of the datasets are different as shown in Figure 5.2, Figure 5.3 and Figure 5.4 on MC, JSRT and Schengen dataset respectively below. This implies the intensity profile variation between datasets can be limit the overall performance of the proposed model.

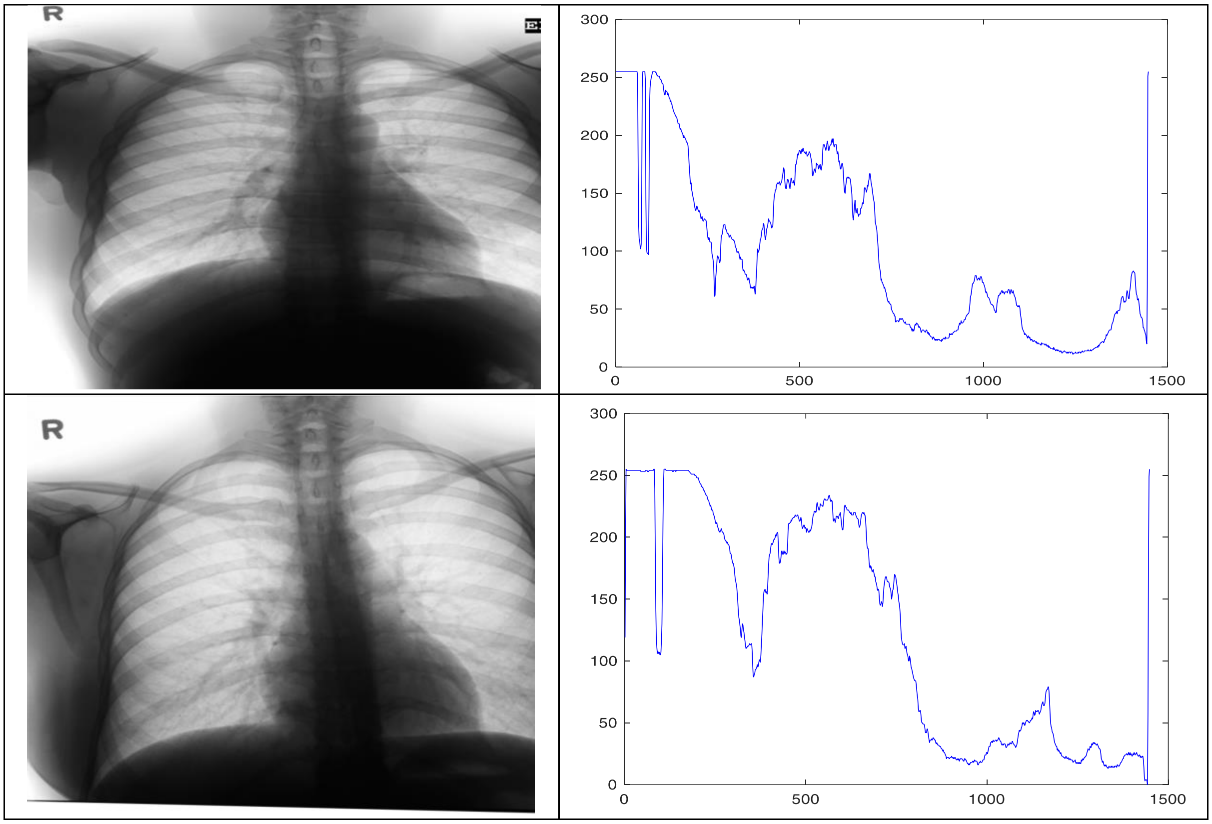

Figure 5.2. Intensity profile on MC dataset sample images

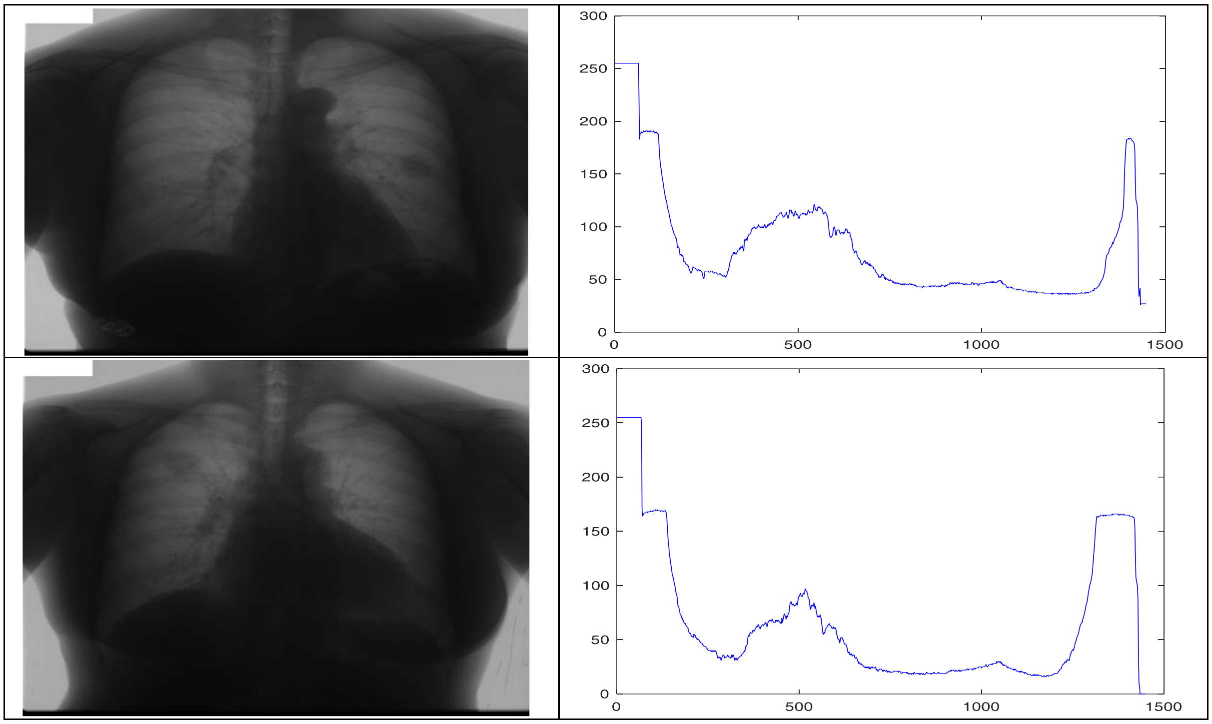

Figure 5.3. Intensity profile on JSRT dataset sample images

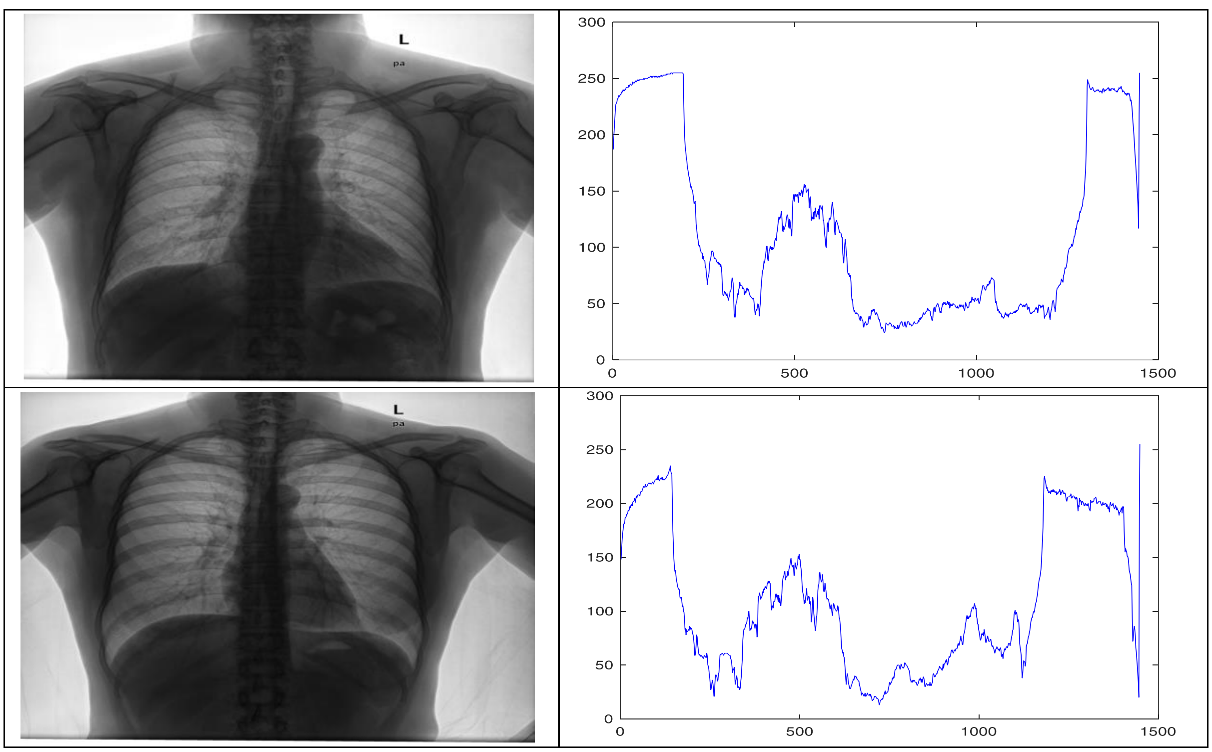

Figure 5.4. Intensity profile on Shenzhen dataset sample images

5.3. Preprocessing

The dataset, image normalization as experienced the limitation in previous chapter, section 4.3, should be standardized. Including the obtained JSRT sliced images, all images are normalized to the size 1024 x 1024 using Matlab built-in imresize function. Subsequently, the removal of

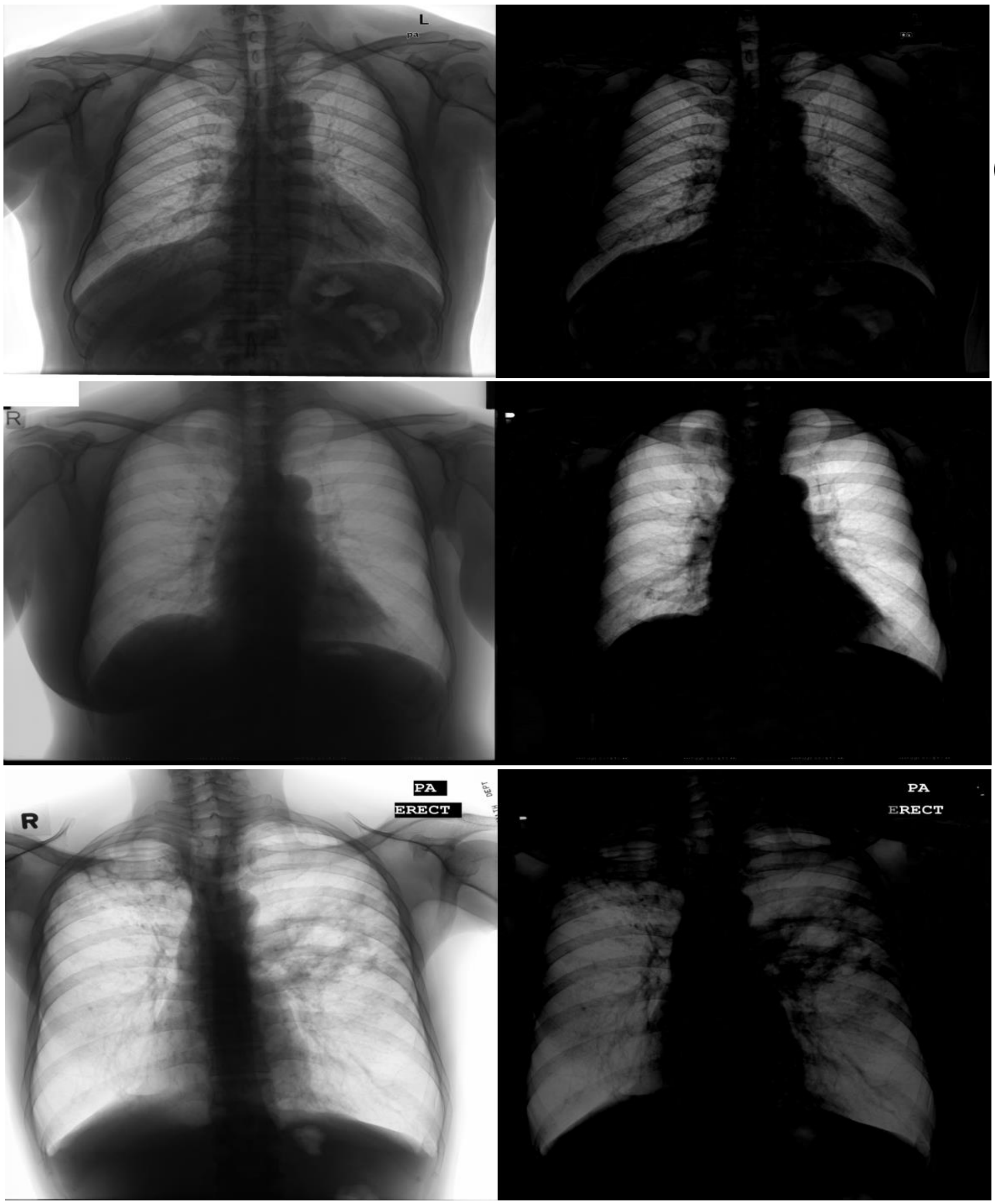

(a)

(b)

(c)

Figure 5.5. Sample image from each dataset

lighter information by considering as background information which are connected with the border is applied. In this case, the Matlab image processing toolbox, explicitly, imclearborder was used with 4 connectivity and the detail implementation code is shown in Appendix: *B*. The sample images are shown in Figure *5.5* after normalization and removal of bordered pixel values. On the specified figure above, the left side column is represents the original image and the right side also the borderless version of each corresponding image (a), (b) and (c) from JSRT, Shenzhen and MC dataset respectively.

By accumulating the preprocessing tasks as described in chapter *4* section *4.4*, the perspective activities are implemented. Thus, with the obtained borderless intensity image from the previous task the intensity image was changed to binary using an imbinarize function with three different threshold values which are 0.01, 0.001, and Otsu threshold algorithm [29] [52] independently. Then, based on best fit selection, the expected lung objects are filtered using Matlab bwareafilt by passing value 2 to select 2 top objects only. Here, the selected objects may contain a hole like area surrounded by somewhere by the object. The hole surrounded by the lung object is definitely the lung part which it may lose its intensity by infection and distortion. To tackle such problems the hole fill function which is imfill is applied. The implementation code for this scenario is shown in Appendix: *C*.

The Figure *5.6* shown below is tabulated as the rows: (1), (2) and (3) are represented sample image from datasets Shenzhen, JSRT and MC respectively and the columns: (a), (b), (c), (d), (e) and (f) are also represented the original image, borderless, binaries then thresholding with local threshold value 0.01, reopen the binary image with two biggest objects among objects, another local threshold value 0.001 and the last one is global Otsu's threshold method i.e. ‘adaptive’ using the same input image respectively.

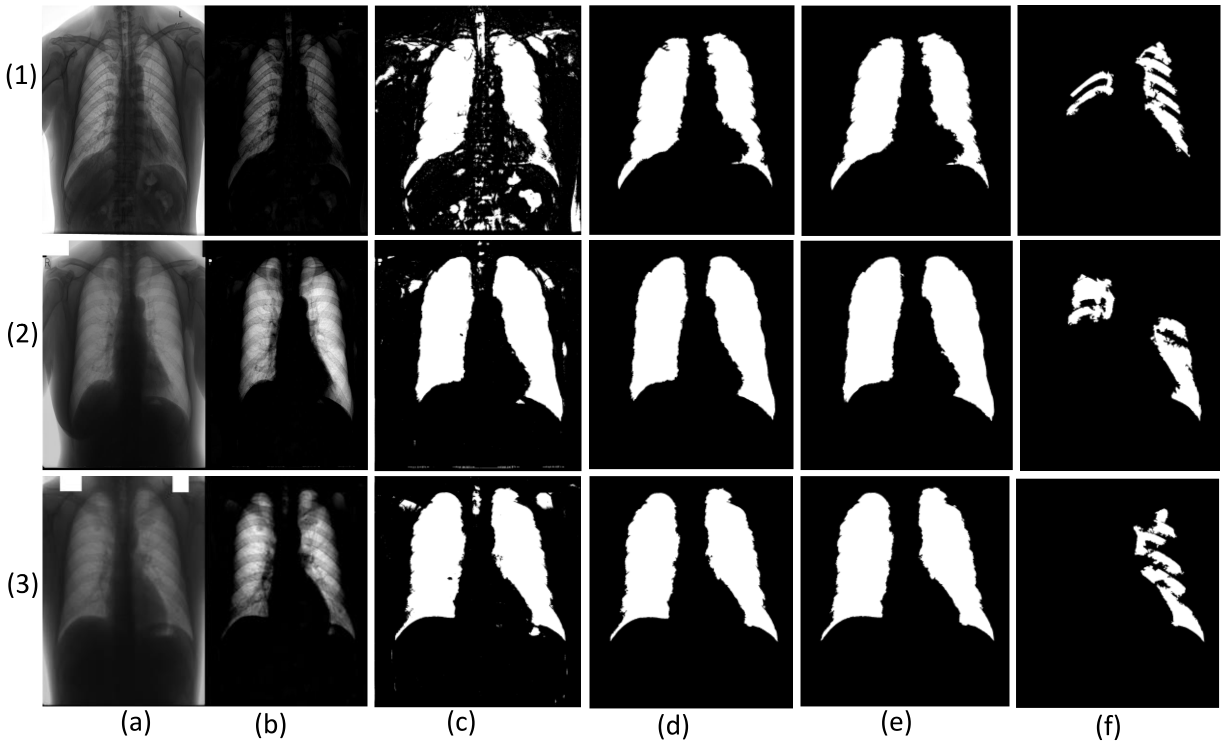

Figure 5.6. Image binarization and thresholding with different threshold values

5.4. Detection of Lung Region

Now the lung objects are clearly identified but the objects' boundary may not sharpen. In order to keep the edge sharpen of the expected lung region, the imdilate is applied as specified the implementation algorithm in Algorithm *4.5* and shown the detail implementation code in Appendix: *D*.

The Figure *5.7* shown below is tabulated as the rows: (1), (2) and (3) are represented sample image from datasets Shenzhen, JSRT and MC respectively and the columns: (a), (b) and (c) are also represented the original image, the detected objects and sharpened or dilated image respectively.

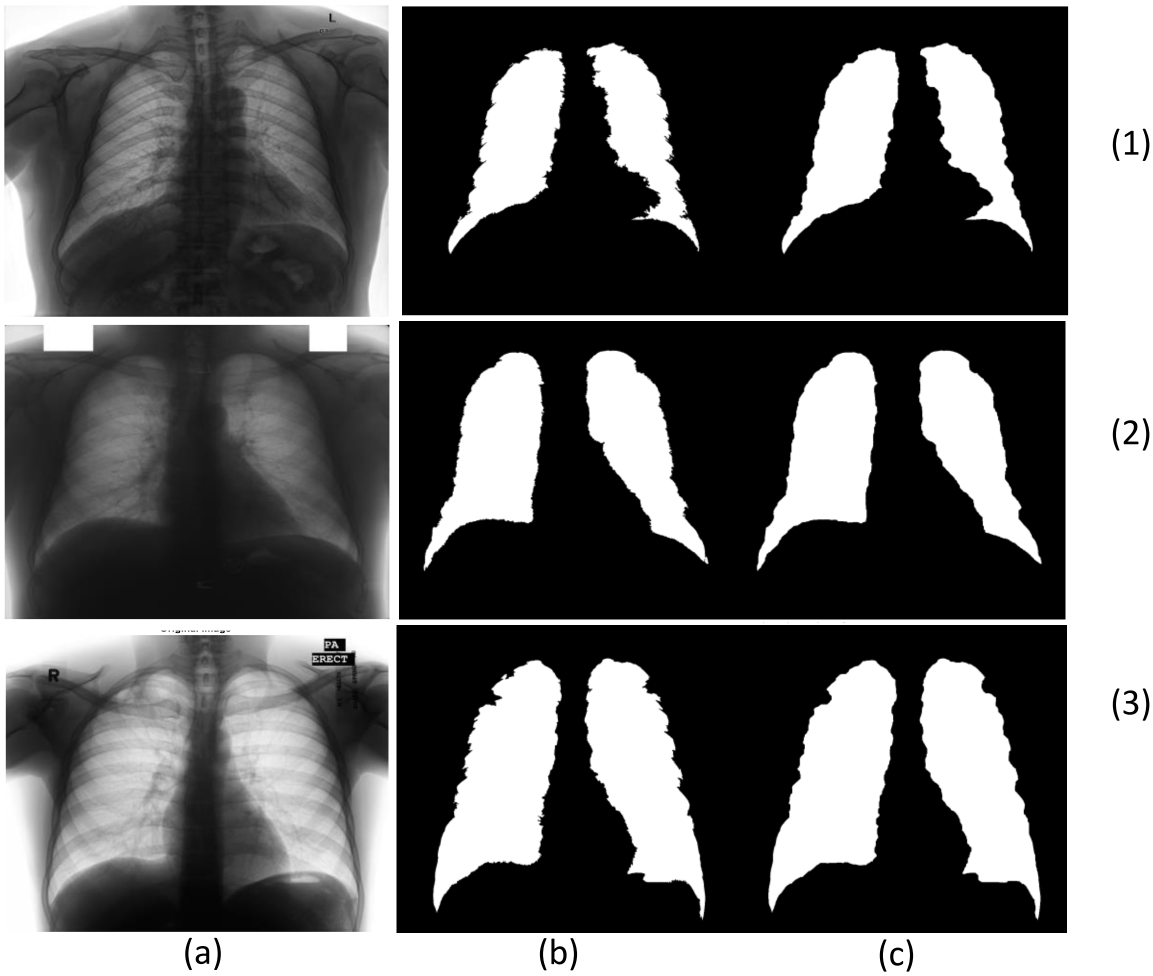

Figure 5.7. Sharpening lung area using image dilation and erosion techniques

5.5. Segmentation

The segmentation is a process of taking the desired object from an object. Shortly, it is a process of filtering desired object and remove unwanted area i.e. treated as background information. The background of detected lung image is in binary format with white color. The aim of the process is extracting the white equivalent region from the original intensity image with the actual intensity value at detected region only otherwise make it 0 or black as stated in Algorithm *4.6* and implementation in Appendix: *D*. The sample segmented image is shown in Figure *5.8* below.

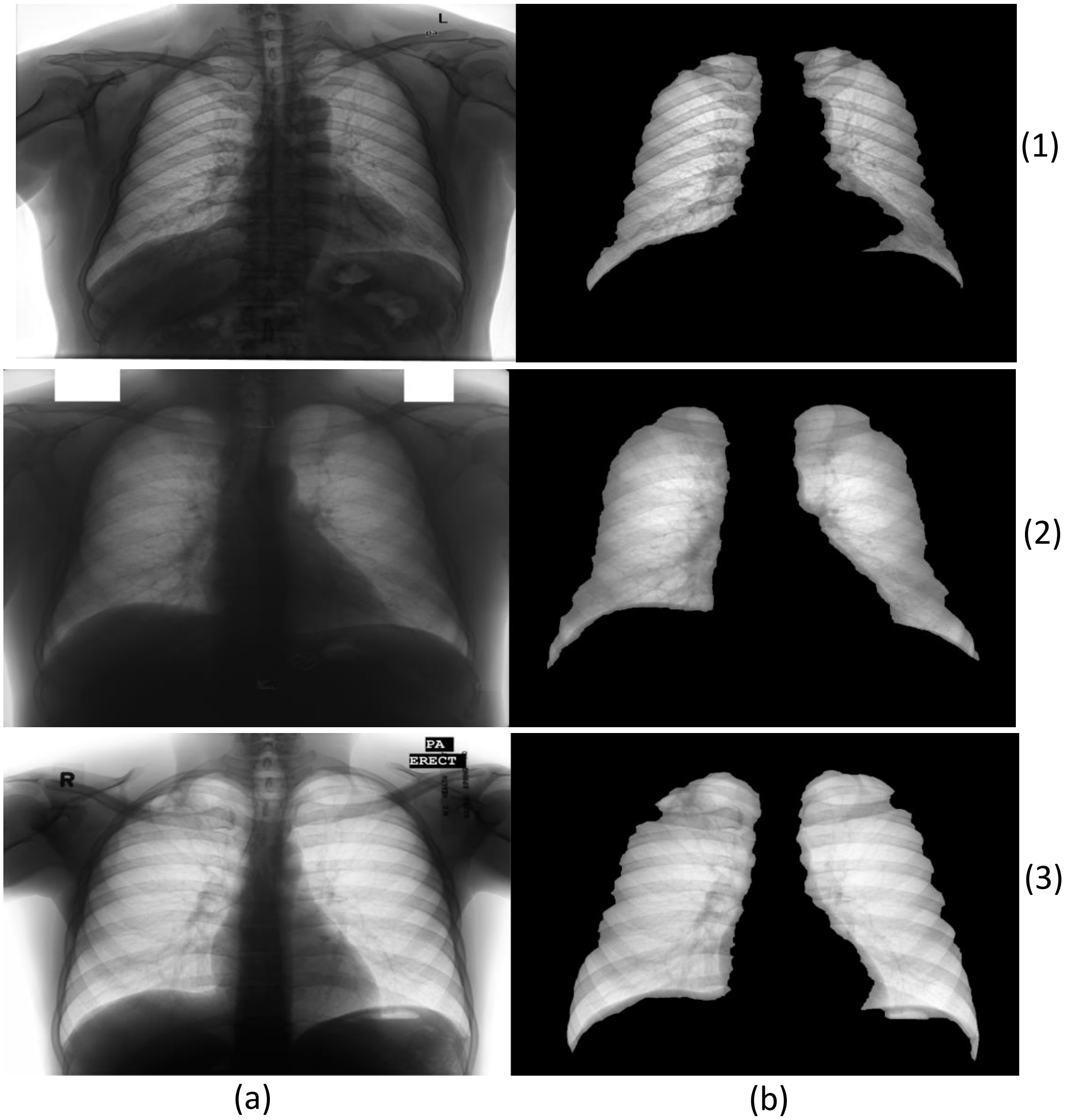

Figure 5.8. Sample segmented images from each dataset

The Figure 5.8 shown above is tabulated as the rows: (1), (2) and (3) are represented sample image from datasets Shenzhen, JSRT and MC respectively and the columns (a) and (b) are also represented the original image and segmented image respectively.

5.6. Feature extraction

In this thesis, the textural feature extraction technique was applied using Matlab image processing toolbox, specifically, graycomatrix which is a GLCM function includes all the four second-order statistics parameters as described in subsection 4.7.1 and Five features from first-order statistics totally 9 parameters were extracted.

During the implementation the first and the second order statistical features were extracted. In the case of the first-order i.e. Kurtosis, skewness, mean, variance and standard deviation and the Matlab hardcode is implemented, calculated, and stored in local permanent storage with excel (.xlsx) format as stated in Appendix: *E* and the second-order or GLCM features are also calculated using Matlab graycomatrix function, the default file type is struct and it needs some conversion task from struct to array then excel as shown the Matlab code in Appendix: *F*. The sample extracted features that are collected from the two methods and the last column named indicator also represents the two classes i.e. normal and abnormal which labeled as 0 and 1 respectively as shown in Figure 5.9 below and Appendix: *G*.

	A	B	C	D	E	F	G	H	I	J	K	L	M	N
1	Mean	STD	Variance	Kurtosis	Skewness	Contrast_LungA	Contrast_LungB	Correlation_LungA	Correlation_Lu	Energy_LungA	Energy_LungB	Homogeneity_Lu	Homogeneity_Lu	Indicator
2	0.801703	0.210457	0.01109	415.9765	-6.24571	0.078465907	0.082901654	0.970828173	0.969179063	0.642606095	0.640978152	0.972199279	0.972442699	0
3	0.82543	0.227558	0.012155	225.3785	-7.16978	0.063610376	0.068326235	0.974756234	0.972884746	0.681749034	0.680331837	0.977455617	0.977410291	0
4	0.778831	0.236393	0.013601	372.9256	-10.0232	0.071795019	0.074104984	0.969787586	0.968815518	0.609417018	0.607893706	0.97086419	0.971416261	0
5	0.792253	0.231673	0.012847	124.2969	-2.9146	0.070129696	0.077092207	0.975311422	0.972860328	0.632309639	0.630383234	0.975167396	0.974639867	0
6	0.758869	0.24077	0.014304	99.97811	-4.85655	0.077790568	0.083933848	0.974369946	0.972345889	0.584956074	0.583378721	0.971935075	0.972073053	0
7	0.788416	0.225239	0.012458	280.9971	-6.42384	0.078039983	0.084662906	0.972141574	0.969777347	0.626338264	0.624631326	0.97260242	0.972700027	0
8	0.743512	0.228463	0.013232	179.3313	-5.24848	0.063621887	0.062965734	0.97111191	0.971409842	0.560485147	0.559486595	0.97095876	0.971467423	0
9	0.826325	0.216961	0.010818	270.5043	-6.07876	0.056732282	0.055611834	0.975274114	0.975762444	0.681674799	0.681019414	0.976366106	0.977328751	0
10	0.804154	0.21892	0.011444	230.4832	-7.07903	0.047594106	0.049148152	0.973463867	0.972597407	0.649269177	0.64785892	0.977863154	0.977121945	0
11	0.857297	0.224601	0.011272	108.859	-4.83975	0.053806454	0.055655961	0.97195637	0.970992418	0.733578698	0.732499465	0.980780588	0.981467758	0
12	0.79551	0.223895	0.012242	251.8641	-6.39153	0.072848317	0.075469092	0.971597163	0.970575349	0.634415232	0.633175515	0.971985198	0.972411921	0
13	0.74681	0.236798	0.013373	249.5024	-9.10593	0.088231457	0.103794943	0.973298872	0.968588958	0.569079965	0.566322679	0.970053033	0.967441132	0
14	0.809267	0.208155	0.010643	201.7783	-5.56495	0.07609071	0.073214765	0.972974289	0.97399576	0.654717788	0.654299179	0.97262992	0.97485179	0
15	0.816236	0.227463	0.012127	251.4172	-5.71216	0.070626607	0.071246307	0.972292034	0.972048915	0.666469836	0.665500312	0.974045349	0.975143334	0
16	0.786554	0.229515	0.012884	515.1321	-8.30419	0.073017152	0.071844902	0.969050628	0.969547503	0.621364137	0.620566467	0.971595328	0.97315457	0
17	0.839931	0.228614	0.011886	396.3559	-9.55878	0.063942289	0.064517862	0.972268464	0.97201884	0.704219769	0.703320374	0.97769432	0.978698454	0
18	0.772927	0.219998	0.012181	292.5407	-7.63806	0.076211581	0.079952803	0.971192263	0.969778092	0.601285603	0.599785542	0.969062008	0.969387527	0
19	0.734484	0.228315	0.012717	119.8843	-4.70869	0.091287748	0.101394804	0.973556834	0.970629141	0.548460059	0.546252997	0.967338888	0.966507585	0
20	[illegible]	[illegible]	[illegible]	[illegible]	[illegible]	[illegible]	[illegible]	[illegible]	[illegible]	[illegible]	[illegible]	[illegible]	[illegible]	0

Figure 5.9. Sample features extracted data

5.7. Classification

The SVM produces hyperplane with principal margin to differentiate samples with in two classes which are either normal or abnormal. In order to classify then train the machine for this study and acquire the SVM classification algorithm, the Matlab Classification Learner is considered. The SVM is used to distinguish incoming instance based on the instance's class that the class was specified by indicator either normal or abnormal i.e. 0 or 1 respectively in to two clusters.

5.8. The Performance Evaluation

Of course in order to evaluate the performance of the proposed model, the dataset should be segmented in to two subset called train and test sets. Using cross-validation [51], the k-folds technique was used i.e. 10-folds, because each instance has a chance to consider as in test and train set on different occasion. In order to implement the performance evaluation of the proposed model, the Matlab classification learner toolbox was adopted to calculate the confusion matrix, sensitivity, specificity and accuracy.

CHAPTER SIX

6. RESULT AND DISCUSSION

6.1. Introduction

Based on the specified solution approach in chapter *4*, in this chapter expected to show step by step events or result during the implementation of the proposed solution staring from image preprocessing to evaluation of the solution. And the triangulation of the solution with others' solutions is another aim of the chapter.

Thus, in this chapter, the obtained results are provided in subsection *6.2* and the triangulation of the final result also discussed in subsection *6.3* below.

6.2. Result

In previous chapter, the implementation of proposed model is done. Of course each major step has its own result then the overall result can be characterized by the performance measurement given below.

The proposed model was implemented using three different public datasets. Each dataset has its own and different intensity value than the others two. This implication gives different results between datasets and a total set also affect the performance of the model. Statistically, *Table 6.1* shows the row facts regarding truly-detected and incorrectly-detected i.e. among 1047 instances 780 instances are detected as same as human expertise and the remaining 267 are detected incorrectly which are from normal and abnormal cases.

When analyzing the true and false detection on each dataset, gives different result and one set can achieve better performance than other due to the variability of the dataset's intensity information. To overcome this problem, the variable thresholding method based on intensity information per CXR image might be needed. The overall performance of the proposed model is relatively low than the current state-of-the-art. But, the lung detection scenario like using manual segmented mask or lung model is improved by this proposed model.

Table 6.1. Confusion matrix of SVM on each dataset

Dataset		**Positive**	**Negative**	**Total**
Shenzhen	**Normal**	280	46	662
	Abnormal	64	272	
JSRT	**Normal**	23	70	247
	Abnormal	20	134	
MC	**Normal**	62	18	138
	Abnormal	26	32	
Total	**Normal**	375	124	1047
	Abnormal	143	405	

Depend on the above statistical information obtained by the SVM classification, the overall performance is better on Schengen dataset, then MC, and JSRT is slightly low than others.

Table 6.2. Classification performance analysis on each dataset

Dataset	AUC	Accuracy (%)	Sensitivity (%)	Specificity (%)
Shenzhen	0.91	83.4	86	81
JSRT	0.62	63.6	25	87
MC	0.71	68.1	78	55
Combined	0.81	74.5	75	74

The following *Figure 6.1* show the overall performance characterized by AUC on Schengen dataset and a red circle like symbol shown in the graph represents the level of the current performance on the dataset.

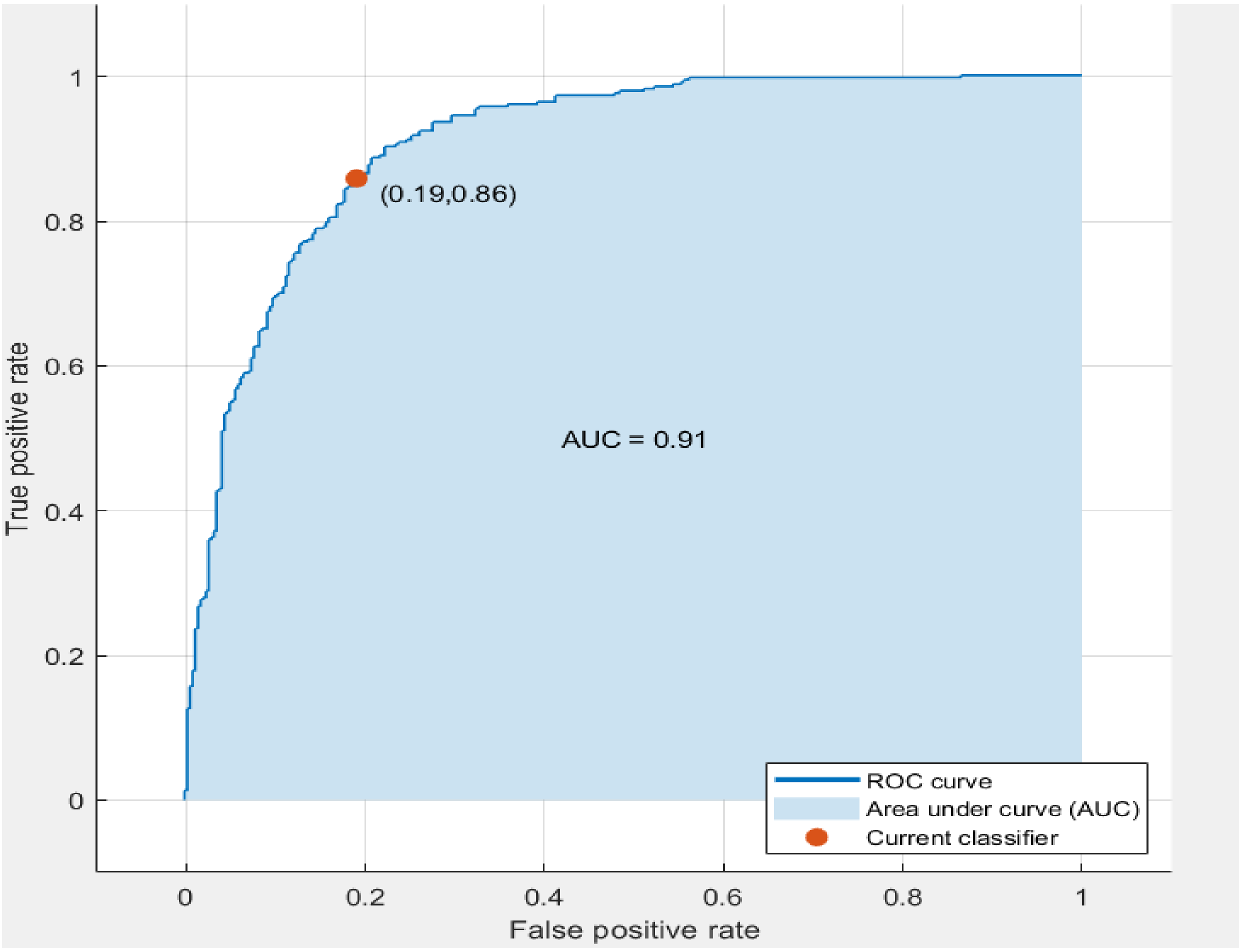

Figure 6.1. AUC on Shenzhen Dataset

The following Figure *6.2* shown the overall performance characterized by AUC on JSRT dataset.

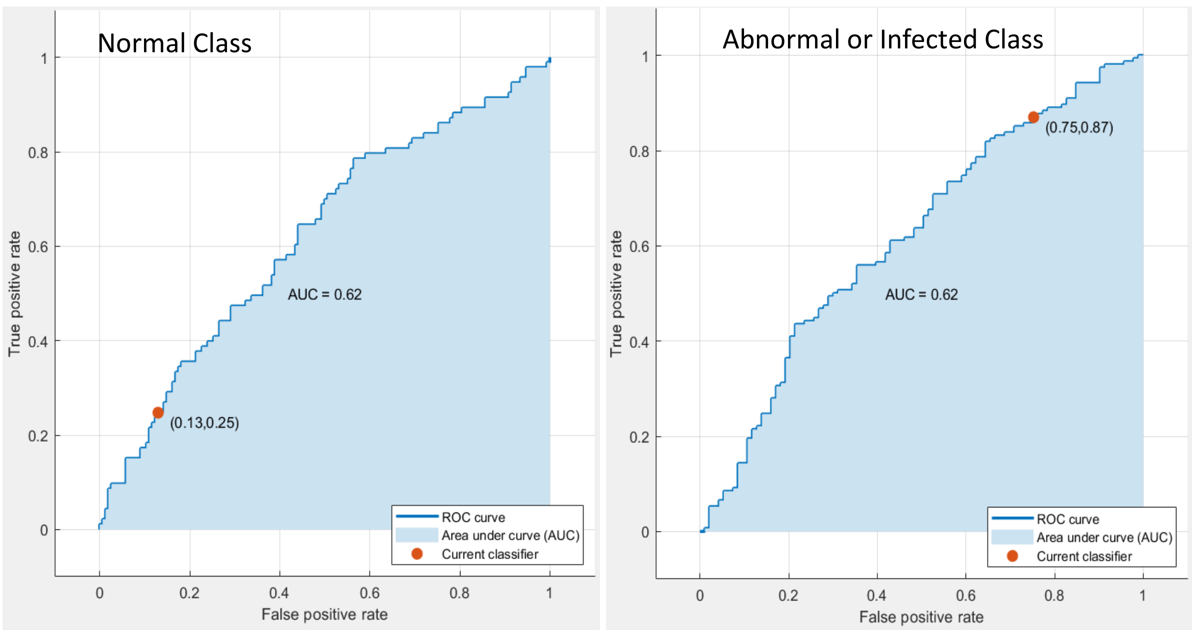

Figure 6.2. Class based AUC on JSRT Dataset

The following Figure *6.3* shown the overall performance characterized by AUC on combined dataset.

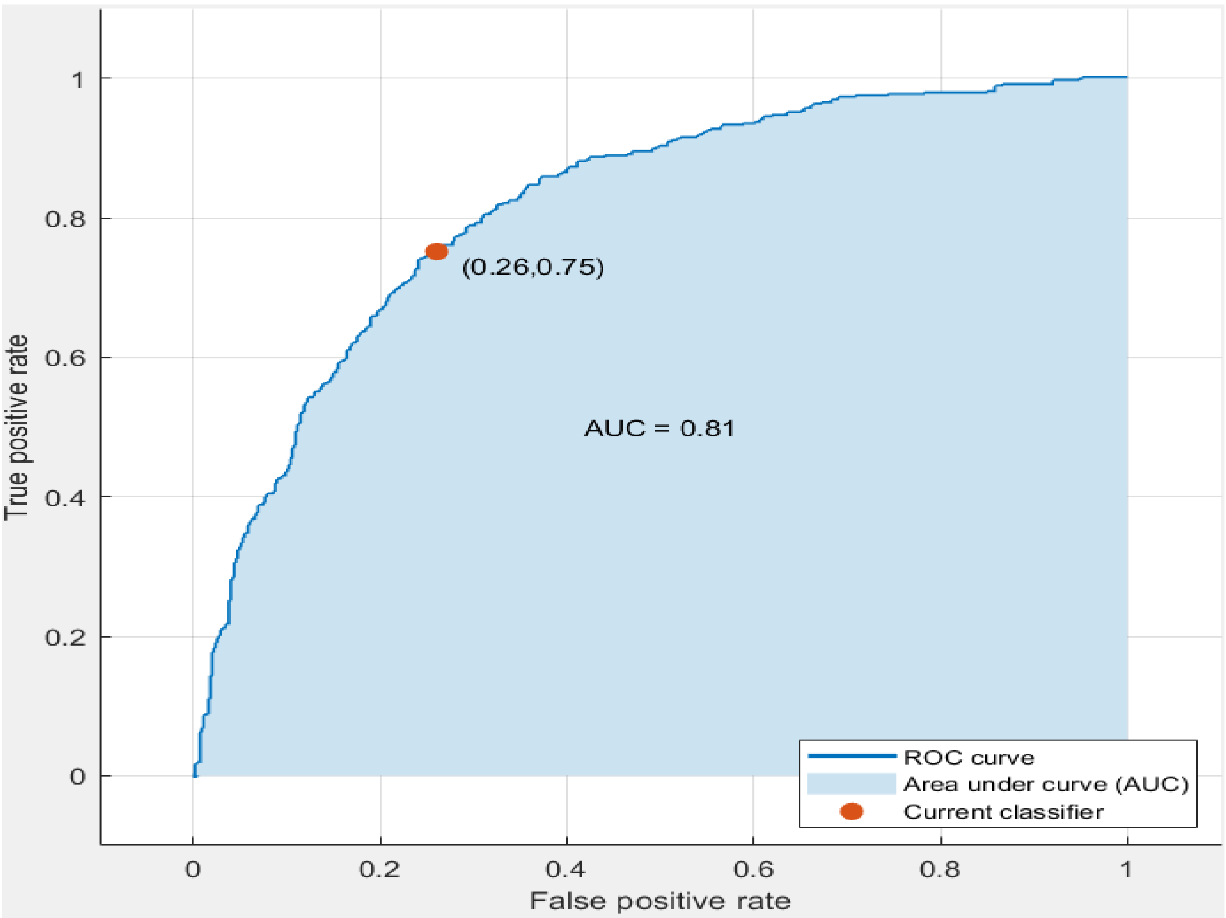

Figure 6.3 AUC on a combination use of all datasets

6.3. Discussion

In this thesis, lung TB detection model in CXR image is proposed. In order to extend the idea, the thesis has three research questions

The result shown above, in terms of achievement in all three datasets are illustrated. Because the last performance result is a sum of all individual result obtained from each DIP task. In order to support lung TB detection in CXR image in health sector, this model is proposed. Based on the survey of the related work, the open issues are identified which may respond by researchers as well.

As s staring point, the thesis has been initiated three research question such that 1) an automatic lung area detection in CXR image, 2) identify the possible feature parameters to be used on classification, and 3) identify possible parameters for performance measurement.

In order to answer the first research question, the lung area is detected using border clearing. Similarly, the selective first-order and second-order statistical parameters are selected. The performance matrix which are accuracy, sensitivity, and specificity are considered.

Unlike other studies reviewed by this thesis, the study is proposed new approach which is an automatic lung area detection. Another technical observation is the variability of intensity profile between datasets that suggests the need of another solution. In order to support this implication, the MC dataset has high intensity profile than Shenzhen and the Shenzhen dataset also has better intensity profile than JSRT dataset as shown in sample images under subsection *5.2*.

CHAPTER SEVEN

7. CONCLUSION AND FUTURE WORK

7.1. Conclusion

TB is one of dominant infectious disease in the world, especially, in developing countries. Like its domination, the detection or diagnosis of TB is tedious step in medical service. When the occurrences of dependent cases like HIV/AIDS, the diagnosis make it more difficult. Nowadays, like any service, medical services are supporting by computer systems, CADe or CADx in medical term with the input of patient medical information and/or medical imaging. The CADx system may accept one or both of the inputs during the implementation.

In order to support lung TB detection in CXR image in health sector, this model is proposed. Based on the survey of the related work, the open issues are identified which may respond by researchers as well. Similarly, the proposed system initiate a novel approach, especially at lung area detection by creating the background portion of CXR image.

By identifying open issues include how detect the lung region automatically, and what are the features can identify a given CXR image is infected or normal are considered using three public datasets such as Schengen, Montgomery Country (MC), and JSRT set a total of 1047 CXR images. As part of model proposal a new approach which is clear the intensities that interconnected with the border CXR image then continue to normal and further processes in image processing. The possible statistical features of a lung object are obtained from the first-order and second-order Gray Level co-occurrence Matrix (GLCM) statistical features. The performance of the proposed model was evaluated using accuracy, sensitivity and specificity. The proposed model was achieved AUC 91%, 62%, 71%, and 81% on Schengen, JSRT, MC and Combined set.

7.2. Future Work

In this study, the automatic TB detection model in CXR image is proposed. One of challenging stage in DIP, in CXR image the lung object detection is achieved with simple processing task i.e. by applying clear border Matlab function. Then, with a local threshold value the lung object was segmented. When checking the performance of the proposed model is different on different datasets. Of course, the lung area detection is possibly identifying, but, the limitation was observed on thresholding on images with different intensity profile as mentioned in subsection 5.2.

The researchers are identified three possible direction as future investigation holes:

1) Develop an algorithm that can segment the lung region from a given CXR image by accumulating variable threshold values between images based on images' intensity information.
2) Between the dataset, the intensity information is different, even if, between images in a dataset. Thus, applying a uniform intensity information between images before applying further DIP task may limit the performance variability between sets and images.
3) When extracting the textural features from the two which are the left and right lung objects, the black area is considered by feature parameters. In order to exclude the background of the image or lung object area, till another open issue identified as future work.

8. REFERENCES

[1] J. O. E. L. D. HOWELL, "EARLY CLINICAL USE OF THE X-RAY," *Trans Am Clin Climatol Assoc,* vol. 127, p. 341–349, 2016.

[2] W. H. Organization, "Global tuberculosis report 2016," World Health Organization, 2016.

[3] M. Klopper, R. M. Warren, C. Hayes, N. C. G. Pittius, E. M. Streicher, B. Muller and others, "Emergence and spread of extensively and totally drug-resistant tuberculosis, South Africa," *Emergence,* 2013.

[4] J. Kasper and F. Bajunirwe, "Brain drain in sub-Saharan Africa: contributing factors, potential remedies and the role of academic medical centres," *Archives of disease in childhood,* pp. archdischild--2012, 2012.

[5] Z. Yousuf, U. Akram, A. Jameel and W. Raza, "Analysis of Tuberculosis Detection Techniques Using Chest X-Rays: A Review," in *2018 IEEE Conference on Systems, Process and Control (ICSPC)*, 2018.

[6] R. H. Cleveland, Imaging in pediatric pulmonology, Springer Science & Business Media, 2012.

[7] S. Raoof, D. Feigin, A. Sung, S. Raoof, L. Irugulpati and E. C. Rosenow III, "Interpretation of plain chest roentgenogram," *Chest,* vol. 141, pp. 545-558, 2012.

[8] J. Corne and K. Pointon, Chest X-Ray Made Easy E-Book, Elsevier Health Sciences, 2009.

[9] K. Siddiqi, M.-L. Lambert and J. Walley, "Clinical diagnosis of smear-negative pulmonary tuberculosis in low-income countries: the current evidence," *The Lancet infectious diseases,* vol. 3, pp. 288-296, 2003.

[10] L.-K. Soh and C. Tsatsoulis, "Texture analysis of SAR sea ice imagery using gray level co-occurrence matrices," *IEEE Transactions on geoscience and remote sensing,* vol. 37, pp. 780-795, 1999.

[11] M. A. Makary and M. Daniel, "Medical error-the third leading cause of death in the US," *BMJ: British Medical Journal (Online),* vol. 353, 2016.

[12] C. Disease Control, Prevention and others, *Core curriculum on tuberculosis: what the clinician should know, Centers for Disease Control and Prevention, Atlanta, GA,* 2015.

[13] S. Jaeger, S. Candemir, S. Antani, Y.-X. J. Wang, P.-X. Lu and G. Thoma, "Two public chest X-ray datasets for computer-aided screening of pulmonary diseases," *Quantitative imaging in medicine and surgery,* vol. 4, pp. 475-477, 2014.

[14] R. C. Gonzalez and R. E. Woods, *Digital Image Processing. Third edit,* New Jersey: Pearson Education, Inc, 2008.

[15] S. J. McPhee, M. A. Papadakis and L. M. Tierney, Current medical diagnosis & treatment 2017, McGraw-Hill Medical New York:, 2017.

[16] B. Starfield, J. Hyde, J. Gervas and I. Heath, "The concept of prevention: a good idea gone astray?," *Journal of Epidemiology & Community Health,* vol. 62, pp. 580-583, 2008.

[17] C. K. Kwan and J. D. Ernst, "HIV and tuberculosis: a deadly human syndemic," *Clinical microbiology reviews,* vol. 24, pp. 351-376, 2011.

[18] H. Communities, "Basics of Tuberculosis," 5 2017. [Online]. Available: http://www.healthcommunities.com/tuberculosis/pathology.shtml.

[19] J. Burrill, C. J. Williams, G. Bain, G. Conder, A. L. Hine and R. R. Misra, "Tuberculosis: A Radiologic Review 1," *Radiographics,* vol. 27, pp. 1255-1273, 2007.

[20] R. Masterclass, "Anatomical Pathology of Tuberculosis," 7 2018. [Online]. Available: https://www.radiologymasterclass.co.uk/.

[21] K. Dheda, M. Ruhwald, G. Theron, J. Peter and W. C. Yam, "Point-of-care diagnosis of tuberculosis: Past, present and future," *Respirology,* vol. 18, pp. 217-232, 2013.

[22] K. D. Toennies, Guide to medical image analysis, Springer, 2017.

[23] W. Gonzalez and R. E. Woods, "Digital image processing using Matlab," *Digital image processing,* 2004.

[24] S. E. Umbaugh, Computer imaging: digital image analysis and processing, CRC press, 2005.

[25] I. Pitas, Digital image processing algorithms and applications, John Wiley & Sons, 2000.

[26] C. Solomon and T. Breckon, Fundamentals of Digital Image Processing: A practical approach with examples in Matlab, John Wiley & Sons, 2011.

[27] D. Sugimura, T. Mikami, H. Yamashita and T. Hamamoto, "Enhancing color images of extremely low light scenes based on RGB/NIR images acquisition with different exposure times," *IEEE Transactions on Image Processing,* vol. 24, pp. 3586-3597, 2015.

[28] V. K. Mishra, S. Kumar and N. Shukla, "Image Acquisition and Techniques to Perform Image Acquisition," *S-JPSET,* 2017.

[29] N. Otsu, "A threshold selection method from gray-level histograms," *IEEE transactions on systems, man, and cybernetics,* vol. 9, pp. 62-66, 1979.

[30] M. Palanivel and M. Duraisamy, "Adaptive Color Texture Image Segmentation Using α-Cut Implemented Interval Type-2 Fuzzy C-Means," *Res. J. Appl. Sci,* vol. 7, pp. 258-265, 2012.

[31] T. M. Mitchell, "Does machine learning really work?," *AI magazine,* vol. 18, pp. 11-11, 1997.

[32] R. O. Duda, P. E. Hart and D. G. Stork, "Pattern classification and scene analysis 2nd ed," *ed: Wiley Interscience,* 1995.

[33] A. Karargyris, J. Siegelman, D. Tzortzis, S. Jaeger, S. Candemir, Z. Xue, K. C. Santosh, S. Vajda, S. Antani, L. Folio and others, "Combination of texture and shape features to detect pulmonary abnormalities in digital chest X-rays," *International journal of computer assisted radiology and surgery,* vol. 11, pp. 99-106, 2016.

[34] S. Candemir, S. Jaeger, K. Palaniappan, J. P. Musco, R. K. Singh, Z. Xue, A. Karargyris, S. Antani, G. Thoma and C. J. McDonald, "Lung segmentation in chest radiographs using anatomical atlases with nonrigid registration," *IEEE transactions on medical imaging,* vol. 33, pp. 577-590, 2014.

[35] M. Kiran, I. Ahmed, N. Khan and A. G. Reddy, "Chest X-ray segmentation using Sauvola thresholding and Gaussian derivatives responses," *Journal of Ambient Intelligence and Humanized Computing,* pp. 1-17, 2019.

[36] N. Singh and S. Hamde, "Tuberculosis Detection Using Shape and Texture Features of Chest X-Rays," in *Innovations in Electronics and Communication Engineering*, Springer, 2019, pp. 43-50.

[37] S. Vajda, A. Karargyris, S. Jaeger, K. C. Santosh, S. Candemir, Z. Xue, S. Antani and G. Thoma, "Feature selection for automatic tuberculosis screening in frontal chest radiographs," *Journal of medical systems,* vol. 42, p. 146, 2018.

[38] S. Rajaraman, S. Candemir, Z. Xue, P. O. Alderson, M. Kohli, J. Abuya, G. R. Thoma and S. Antani, "A novel stacked generalization of models for improved tb detection in chest radiographs," in *2018 40th Annual International Conference of the IEEE Engineering in Medicine and Biology Society (EMBC)*, 2018.

[39] S. Jaeger, O. H. Juarez-Espinosa, S. Candemir, M. Poostchi, F. Yang, L. Kim, M. Ding, L. R. Folio, S. Antani, A. Gabrielian and others, "Detecting drug-resistant tuberculosis in chest radiographs," *International journal of computer assisted radiology and surgery,* vol. 13, pp. 1915-1925, 2018.

[40] R. J. Wieringa, Design science methodology for information systems and software engineering, Springer, 2014.

[41] P. Soille, Morphological image analysis: principles and applications, Springer Science & Business Media, 2013.

[42] D. Bradley and G. Roth, "Adaptive thresholding using the integral image," *Journal of graphics tools,* vol. 12, pp. 13-21, 2007.

[43] R. Van Den Boomgaard and R. Van Balen, "Methods for fast morphological image transforms using bitmapped binary images," *CVGIP: Graphical Models and Image Processing,* vol. 54, pp. 252-258, 1992.

[44] R. M. Haralick, K. Shanmugam and others, "Textural features for image classification," *IEEE Transactions on systems, man, and cybernetics,* pp. 610-621, 1973.

[45] M. Tuceryan and A. K. Jain, "The Handbook of Pattern Recognition and Computer Vision , chapter 2.1," *Texture Analysis. World Scientific Co.,,* pp. 207-248, 1998.

[46] P. S. Hiremath and J. Pujari, "Content Based Image Retrieval based on Color, Texture and Shape features using Image and its complement," *International Journal of Computer Science and Security,* vol. 1, pp. 25-35, 2007.

[47] M. Tsaneva, "Texture features for segmentation of satellite images," *Cybernetics and Information Technologies,* vol. 8, pp. 73-85, 2008.

[48] S. D. Newsam and C. Kamath, "Comparing shape and texture features for pattern recognition in simulation data," in *Image Processing: Algorithms and Systems IV*, 2005.

[49] S. B. Kotsiantis, I. D. Zaharakis and P. E. Pintelas, "Machine learning: a review of classification and combining techniques," *Artificial Intelligence Review,* vol. 26, pp. 159-190, 2006.

[50] M. A. Hearst, S. T. Dumais, E. Osuna, J. Platt and B. Scholkopf, "Support vector machines," *IEEE Intelligent Systems and their applications,* vol. 13, pp. 18-28, 1998.

[51] G. H. Golub, M. Heath and G. Wahba, "Generalized cross-validation as a method for choosing a good ridge parameter," *Technometrics,* vol. 21, pp. 215-223, 1979.

[52] P. A. Cheremkhin and E. A. Kurbatova, "Comparative appraisal of global and local thresholding methods for binarisation of off-axis digital holograms," *Optics and Lasers in Engineering,* vol. 115, pp. 119-130, 2019.

APPENDIXES

Appendix: A Image Slicing (Matlab Code)

```
%%This implementation used to convert multiple (#247) JSRT IMG to PNG image format
folder='D:\Academic\My Thesis Set\Dataset\All247images'; %Load images' directory
srcFiles = dir(fullfile(folder, '*.IMG')); %Read all IMG files in the directory
len=length(srcFiles); % count number of IMG files in the directory
for i = 1 : len
    filename = fullfile(folder, srcFiles(i).name); %Read the full path with the name
    fid = fopen( filename,'r','b'); %Open for reading and r and b specifies for reading
                                    % and IEEE floating point respectively
    oneSlice = fread(fid, [2048 2048], '2*uint16','b');%Read binary data from file fid
                                                        %with four parameters i.e. the
                                                        %file, size, precision and format
    img = mat2gray(oneSlice, [0,4096]); %Convert the matrix to intensity image
    fclose(fid);              %Closes open file fid
    imgR = imrotate(img,270); %Rotate the image to normal position
    imgR = flip(imgR, 2);     %Flip to mirror view
    imwrite(imgR,sprintf('JPCNN%03d.png',i));%Save the image with prefix JPCNN and
                                              % successive i value format like 001, 002…
end
```

Appendix: B Image Normalization and Removal of bordered pixel values

```
%%This implementation is used to normalize the CXR images and remove the background info

folder='D:\Academic\A Matlab 1\TotalSet'; %Load images' directory
files = dir(fullfile(folder, '*.PNG')); %Read all PNG files in the directory
len=length(srcFiles); % count number of PNG files in the directory

for i = 1: len

    image=imread(fullfile(folder, files(i).name)); %Read the image listed in i
    image=imresize(image, [1024 1024]); %Resize the image in to 1024x1024 resolution
    image=imclearborder(image,4); %Clear the background information which connected
                                  %with the border of image and 4 connectivity
    imwrite(image, sprintf(files(i).name));% save inside current location

end
```

Appendix: C A Matlab code for image binarization and thresholding

```
%% Matlab code for image binarization, thresholding with different
%threshold methods using global and local threshold values
folder='D:\Academic\My Thesis Set\Dataset\Process1'; %Load images' directory
files = dir(fullfile(folder, '*.PNG')); %Read all PNG files in the directory
len=length(files); % count number of PNG files in the directory
for kl=1:len
    image=imread(fullfile(folder, files(kl).name)); %Read the image listed in kl
     im_one=imbinarize(image, 0.01);%convert the image into binary form then
                                     %use threshold value 0.01 is used as Method 1
     im_one =bwareafilt(im_one,2); %select top two objects from the image im_one
     im_one =imfill(im_one,'holes'); %fill black portion of the selected objects

     im_two=imbinarize(image, 0.001);%convert the image into binary form then
                                     %use threshold value 0.001 is used as Method 2
     im_two =bwareafilt(im_two,2); %select top two objects from the image im_two
     im_two =imfill(im_two,'holes'); %fill black portion of the selected objects

     im_three=imbinarize(image, 'adaptive');%convert the image into binary form
                                     %use threshold method Otsu is used as Method 3
```

```
    im_three =bwareafilt(im_three,2); %select top two objects from the image
    im_three =imfill(im_three,'holes');%fill black portion of the selected obj
    imwrite(im_one, sprintf(files(kl).name));% save inside current location
    imwrite(im_two, sprintf(files(kl).name));% save inside current location
    imwrite(im_three, sprintf(files(kl).name));% save inside current location
end
```

Appendix: D A Matlab code for segmentation

```
%%Segmentation by determining columns and rows
folder='D:\Academic\My Thesis Set\Dataset\Process2'; %Load detected lung area images
folder1='D:\Academic\My Thesis Set\Dataset\TotalSet'; %Load images' directory

files = dir(fullfile(folder, '*.PNG')); %Read all PNG files in the directory

len=length(files); % count number of PNG files in the directory

for i=1:len
     im=files(i).name;  %name of the image
     image1=imread(fullfile(folder,im)); %Read detected lung area
     image2=imread(fullfile(folder1,im)); %Read original image
     for m=1:1024
         for n=1:1024
             if image1(m,n)==0
                 image2(m,n)=0;
             end
         end
     end
     imwrite(image2, sprintf(files(i).name));%Save inside current location
end
```

Appendix: E   A Matlab code for Extracting First-Order Statistics

```
%% Statistical feature are extracted using First-Order statistical parameters
% which are Min, Max, Mean, Std, Var, Kurtosis and Skewness;
folder='D:\Academic\My Thesis Set\Dataset\Process3'; %Load segmented images
files = dir(fullfile(folder, '*.PNG')); %Read all PNG files in the directory

len=length(files); % count number of IMG files in the directory
for i=1:len
    im2=files(i).name; %name of the image
    image=imread(fullfile(folder,im2)); %Read the segmented image i
    Min=min(min(im2double(image)));       % Min, double min function in 2d image
    Max=max(max(im2double(image)));       % Max
    Mean=mean(mean(im2double(image)));    % Mean
    Std=std(std(im2double(image)));       % standard deviation std
    Var=var(var(im2double(image)));    % The Variance
    Kurtosis=kurtosis(kurtosis(im2double(image))); % The Kurtosis
    Skewness=skewness(skewness(im2double(image))); % Skewness
    c=[Min Max Mean Std Var Kurtosis Skewness];%Populate a matrix of 5 parameters
end
xlswrite('First-Order',c); %save in to local disk with excel format xlsx
```

Appendix: F A Matlab code for Extracting Second-Order statistical features using GLCM

```
%% Calculate the four second-order statistical features using built-in GLCM
% function
folder='D:\Academic\My Thesis Set\Dataset\Process3'; %Load segmented images
files = dir(fullfile(folder, '*.PNG')); %Read all PNG files in the directory

len=length(files); % count number of PNG files in the directory
for km=1:len
    im2=files (km).name; %name of the image
    image=imread(fullfile(folder,im2)); %Read the segmented image i
    GLCM2 = graycomatrix(image,'Offset');%offset represents→neighbor
                                          %[0, 1] is default
              %Populate a matrix of 4 GLCM parameters below at specified list km
    st3{km} = graycoprops(GLCM2,{'Contrast','Correlation','Energy','Homogeneity'});
end
    ds2=struct2table(st3{1,1});%Convert the first list in structure to normal
                               %table form
for io=2:len %Convert a list in structure to normal table form from 2nd to len
              %records
     ds2=[ds2; struct2table(st3{1,io})];
end
filename = 'Second_Order.xlsx';
writetable(ds2,filename); %save in to local disk with excel format xlsx
```

Appendix: G Sample Data on Feature Extraction

	A	B	C	D	E	F	G	H	I	J	K	L	M	N
1	Mean	STD	Variance	Kurtosis	Skewness	Contrast_LungA	Contrast_LungB	Correlation_LungA	Correlation_Lu	Energy_LungA	Energy_LungB	Homogeneity_Lu	Homogeneity_Lu	Indicator
2	0.801703	0.210457	0.01109	415.9765	-6.24571	0.078465907	0.082901654	0.970828173	0.969179063	0.642606095	0.640978152	0.972199279	0.972442699	0
3	0.82543	0.227558	0.012155	225.3785	-7.16978	0.063610376	0.068326235	0.974756234	0.972884746	0.681749034	0.680331837	0.977455617	0.977410291	0
4	0.778831	0.236393	0.013601	372.9256	-10.0232	0.071795019	0.074104984	0.969787586	0.968815518	0.609417018	0.607893706	0.97086419	0.971416261	0
5	0.792253	0.231673	0.012847	124.2969	-2.9146	0.070129696	0.077092207	0.975311422	0.972860328	0.632309639	0.630383234	0.975167396	0.974639867	0
6	0.758869	0.24077	0.014304	99.97811	-4.85655	0.077790568	0.083933848	0.974369946	0.972345889	0.584956074	0.583378721	0.971935075	0.972073053	0
7	0.788416	0.225239	0.012458	280.9971	-6.42384	0.078039983	0.084662906	0.972141574	0.969777347	0.626338264	0.624631326	0.97260242	0.972700027	0
8	0.743512	0.228463	0.013232	179.3313	-5.24848	0.063621887	0.062965734	0.97111191	0.971409842	0.560485147	0.559486595	0.97095876	0.971467423	0
9	0.826325	0.216961	0.010818	270.5043	-6.07876	0.056732282	0.055611834	0.975274114	0.975762444	0.681674799	0.681019414	0.976366106	0.977328751	0
10	0.804154	0.21892	0.011444	230.4832	-7.07903	0.047594106	0.049148152	0.973463867	0.972597407	0.649269177	0.64785892	0.977863154	0.977121945	0
11	0.857297	0.224601	0.011272	108.859	-4.83975	0.053806454	0.055655961	0.97195637	0.970992418	0.733578698	0.732499465	0.980780588	0.981467758	0
12	0.79551	0.223895	0.012242	251.8641	-6.39153	0.072848317	0.075469092	0.971597163	0.970575349	0.634415232	0.633175515	0.971985198	0.972411921	0
13	0.74681	0.236798	0.013373	249.5024	-9.10593	0.088231457	0.103794943	0.973298872	0.968588958	0.569079965	0.566322679	0.970053033	0.967441132	0
14	0.809267	0.208155	0.010643	201.7783	-5.56495	0.07609071	0.073214765	0.972974289	0.97399576	0.654717788	0.654299179	0.97262992	0.97485179	0
15	0.816236	0.227463	0.012127	251.4172	-5.71216	0.070626607	0.071246307	0.972292034	0.972048915	0.666469836	0.665500312	0.974045349	0.975143334	0
16	0.786554	0.229515	0.012884	515.1321	-8.30419	0.073017152	0.071844902	0.969050628	0.969547503	0.621364137	0.620566467	0.971595328	0.97315457	0
17	0.839931	0.228614	0.011886	396.3559	-9.55878	0.063942289	0.064517862	0.972268464	0.97201884	0.704219769	0.703320374	0.97769432	0.978698454	0
18	0.772927	0.219998	0.012181	292.5407	-7.63806	0.076211581	0.079952803	0.971192263	0.969778092	0.601285603	0.599785542	0.969062008	0.969387527	0
19	0.734484	0.228315	0.012717	119.8843	-4.70869	0.091287748	0.101394804	0.973556834	0.970629141	0.548460059	0.546252997	0.967338888	0.966507585	0
20	0.708171	0.220379	0.012159	270.6198	-7.75858	0.07009708	0.071213691	0.975203071	0.974808068	0.50875331	0.507047391	0.965899236	0.965488022	0
21	0.713155	0.217564	0.012023	323.5931	-4.87654	0.127113311	0.134632209	0.979857201	0.978665732	0.510972003	0.509660562	0.954555578	0.954263779	0
22	0.754585	0.2274	0.012767	222.6836	-7.76777	0.084411573	0.087834312	0.972490298	0.971374829	0.575201315	0.57387121	0.970383507	0.971019435	0
23	0.747555	0.228051	0.012876	287.2953	-7.59503	0.075236944	0.08487395	0.972087865	0.968512635	0.564099315	0.561481833	0.970007067	0.967509881	0
24	0.774778	0.235161	0.01334	343.521	-9.31986	0.081806147	0.092634588	0.97131507	0.967518129	0.60732064	0.605079966	0.971189549	0.970248008	0
25	0.770554	0.234783	0.013339	471.418	-8.28645	0.074538583	0.079985419	0.973767909	0.971851024	0.599116789	0.597407273	0.971168924	0.971183553	0
26	0.710321	0.236051	0.013824	383.8536	-7.48196	0.084776102	0.093340624	0.973691832	0.971034044	0.51729598	0.515114859	0.964801491	0.963667613	0
27	0.78955	0.210945	0.010873	493.6136	-8.0277	0.072692913	0.074325621	0.973974179	0.97338963	0.62534995	0.624375502	0.97328879	0.9743269	0
28	0.838111	0.226663	0.01215	235.0297	-5.10524	0.065488661	0.071192587	0.971337626	0.968841193	0.702337623	0.700813393	0.979400717	0.978547654	0